

**FEASIBILITY INVESTIGATION OF THE
GIROMILL
FOR GENERATION OF ELECTRICAL
POWER**

VOLUME II - TECHNICAL DISCUSSION

Final Report for the
Period April 1975 - April 1976

R.V. Brulle

MCDONNELL AIRCRAFT COMPANY
Box 516
St. Louis, Missouri 63166

Date Published - January 1977

PREPARED FOR THE UNITED STATES
ENERGY RESEARCH AND DEVELOPMENT ADMINISTRATION
DIVISION OF SOLAR ENERGY

Under Contract No. EY-76C-02-2617.A001

FOREWORD

This report was prepared for the United States Energy Research and Development Administration (ERDA) by the McDonnell Aircraft Company (MCAIR), a division of the McDonnell Douglas Corporation, P. O. Box 516, St. Louis, Missouri, 63166. This study was performed under ERDA contract E(11-1)-2617.

This final report covers the results obtained over the entire contract period from 1 April 1975 to 30 April 1976. However, emphasis is given to the period subsequent to the publication of our mid-term report on 1 November 1975. The pertinent results from the mid-term are summarized so that this final report is complete and can stand alone. In addition, the contents of this report are arranged in the same order as our mid-term to make cross checking and referencing between them convenient. The report is in two volumes. Volume I is an Executive Summary and Volume II the Technical Discussion.

The study was under the direction of Robert V. Brulle. Contributing personnel were: William E. Simon and R. D. Turner, aerodynamics and performance; Thomas V. Hinkle and Anthony R. Dill, structural strength analysis; Rudy N. Yurkovich, structural dynamics; Bruno Fajfar, control system; Fred R. Cole and John J. Blommer, design; Robert A. Juergens, electronics; and James H. Carlson, costs.

ABSTRACT

The Giromill (from cyclogiro windmill) consists of a number of vertical blades rotating around a central tower. The blades' angle of attack are individually modulated to achieve high wind energy conversion efficiency. This one year study concentrated on determining the feasibility of the Giromill for the cost effective production of electrical energy.

Twenty-one different Giromill configurations covering three sizes of Giromill systems (120, 500, and 1500 kW) were analyzed, varying such parameters as rotor solidity, rotor aspect ratio, rated wind velocity, and number of rotor blades. The Giromill system analysis employed the same ground rules being used for conventional windmill analyses to facilitate comparisons between these systems.

The results indicate that a Giromill is a very efficient device, and coupled with its relatively simple construction appears quite cost effective when compared to conventional windmills. A 500 kW Giromill system, placed in a 5.4 mps mean wind site, can generate electrical power for 4.05¢ per kW hr. which is 18 to 39% less than that of conventional windmills. Further effort to verify the analytical performance with a wind tunnel test is recommended.

TABLE OF CONTENTS

<u>Section</u>	<u>Page</u>
1. INTRODUCTION	1
2. STUDY GROUND RULES	2
2.1 Summary	2
2.2 Optimum Giromill Design	3
3. AERODYNAMICS AND PERFORMANCE	4
3.1 Aerodynamic Analysis	4
3.2 Performance	8
4. GIROMILL SYSTEM DESIGN	12
5. STRUCTURAL/STRENGTH DESIGN	18
5.1 Structural Arrangement	18
5.2 Structural Design	20
5.2.1 Blade Design	21
5.2.2 Blade Supports and Tower Design	21
5.3 Structural Sizing Results	22
5.4 Configuration 11-1 Structural Analysis	22
5.5 Structural Dynamics	26
5.5.1 Structural Dynamics Analysis Overview	26
5.5.2 Configuration 11-1 Structural Dynamics	29
6. CONTROL SYSTEM	31
6.1 Control System Functional Operation	31
6.2 Blade Rock Angle Control Implementation	31
6.3 Effect of Aerodynamic Net Torque Variation on Rotor RPM	38
7. ENERGY OUTPUT EVALUATION	41
7.1 Wing Duration Curves	41
7.2 Energy Output	42
8. COST ANALYSIS	43
8.1 Basic Cost Elements	44
8.2 Production Costs for Giromill Subsystems	46
8.3 Total Giromill System Cost	53
8.4 Optimized System Cost	55
8.5 Cost Comparison with Conventional Windmills	61
9. CONCLUSIONS	63
APPENDIX A	64
REFERENCES	67

List of Figures

<u>Figure</u>	<u>Title</u>	<u>Page</u>
1	Ground Rules Summary	2
2	Giromill Study Configurations	3
3	Cyclogiro Rotor Parameters Definition	5
4	Two-Dimensional (Section) Aerodynamic Characteristics Used for Performance Calculations	6
5	Airfoil Section Characteristics Used for Performance Calculations	7
6	Giromill Performance Characteristics	8
7	Performance Envelope Comparison	9
8	α_e for $C_{P_{MAX}}$ at High λ	9
9	$C_{P_{MAX}}$ and Corresponding α_e	10
10	Angle of Attack Profile	10
11	Giromill Power	11
12	Giromill Configuration	12
13	Conceptual Designs Investigated	13
14	500 kw Giromill Configuration 11-1	15
15	Blade Concepts Investigated	16
16	Blade Rock Angle Actuator	17
17	Giromill Geometric Data and Design Weights	23
18	Blade Limit Loads	24
19	Tower Limit Loads - Operating Condition	25
20	Configuration 11 and 11-1 Structural Weights	26
21	Summary of Structural Dynamics Frequencies	29
22	Tower Dynamics	30
23	Giromill Control System Functional Diagram	32
24	Blade Rock Angle Control Functional Representation	34
25	Blade Rock Control Implementation	35
26	Induced Angle of Attack Along the Blade Orbit	37
27	Induced Angle of Attack Coefficient Variation with Wind Velocity Ratio	37
28	Rock Angle Computation Comparison	38
29	Cyclic Torque Variation	39
30	Rotor Angular Velocity Variation	40
31	Uprated Wind Speed Duration Curves	41
32	Cost of Capital Analysis for Typical Capital Structure	45
33	Cost Relationship for 100 to 150 kw Synchronous Generator	48
34	Cost Relationship for 500 kw Synchronous Generator	48
35	Cost Relationships for 100 to 150 kw and 500 kw Speed Increases	49
36	Cost Relationship for Flexible Coupling	50
37	Cost Relationship for Large Diameter Combination Bearing	50
38	Cost Relationship for Small Diameter Combination Bearings	51
39	Mechanical Power Transmission Components and Character- istics	52
40	Estimated Costs for Rotor Blade Actuators	53
41	Cost Estimating Relationships Summary	54

List of Figures (Continued)

<u>Figure</u>	<u>Title</u>	<u>Page</u>
42	120 kw and 500 kw Giromill System Costs	56
43	Production Cost Elements for 1500 kw Configurations	57
44	Cost of Energy Produced for 1500 kw Configurations	58
45	500 kw Configuration 11-1 Cost Analysis	59
46	Cost of Energy Produced 500 kw Configuration 11-1	60
47	Giromill and Conventional Windmill Cost Comparison	61
48	Energy Costs Comparison for a Consistant Command Charge	62

1. INTRODUCTION

Wind energy has been used for centuries as a source of power on a small scale. To become a significant contribution to the nation's energy needs, wind energy extraction devices will have to be developed on a scale that would entail a very large capital investment. The most effective system must be identified before such a commitment can be undertaken.

One such device that offers considerable promise is the Giromill. It consists of a number of vertical blades rotating around a central tower. The blades angle of attack are individually modulated to achieve high wind energy conversion efficiency regardless of the wind direction. Compared to conventional windmills, tower and blade construction are considerably simplified.

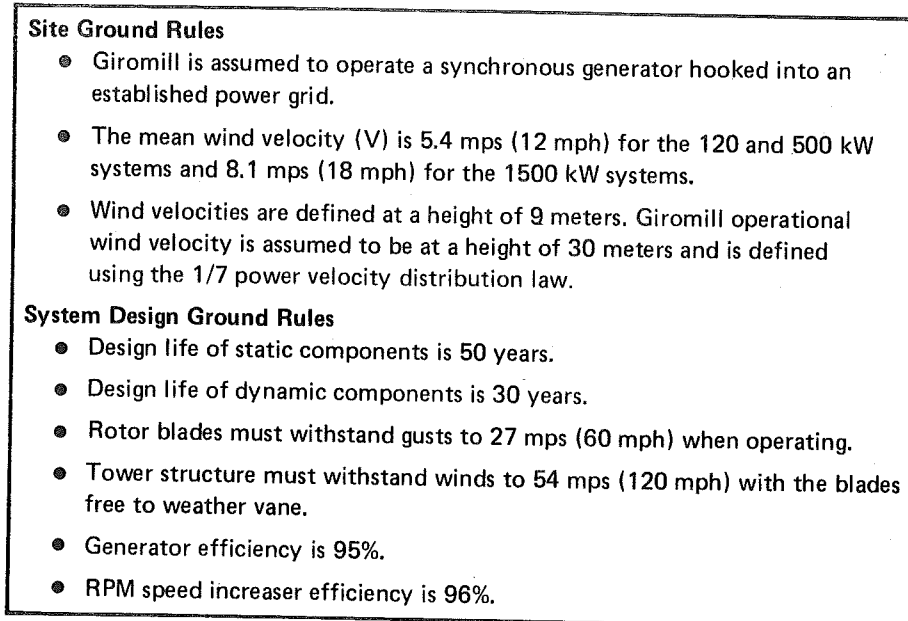
This study concentrated on identifying the potential advantages and problem areas of the Giromill, and defining its cost effectiveness for comparison to more conventional systems being studied elsewhere. The initial emphasis of the study during the first six months was directed towards a parametric evaluation of the Giromill system. The results of this evaluation provided an understanding of the Giromill system and identified the major cost components. The latter part of the study was devoted to a more detailed investigation and cost optimization of the most promising Giromill system and preparation of a wind tunnel test plan. The results from this one year study have verified the Giromill feasibility and its cost effectiveness such that further effort to verify the theoretical performance is warranted.

This report presents the study analysis results, and together with the mid-term report (Reference 1) provides all of the data, rationale, and techniques used to arrive at these results.

2. STUDY GROUND RULES

2.1 Summary

The purpose of this study was to determine the feasibility of the Giromill for the cost effective production of electrical energy. Study ground rules employed by General Electric and Kaman for analysis of conventional windmills were used as a guide to facilitate comparison of our Giromill results with conventional windmills. The more pertinent site and system design ground rules used are shown in Figure 1. Cost ground rules are discussed in Section 8.



GP77-0007-35

**FIGURE 1
GROUND RULES SUMMARY**

Three sizes of Giromill systems were analyzed. They were: 120, 500, and 1500 kW systems. The 120 and 500 kW systems were sized to operate in a 5.4 mps (12 mph) mean wind site, and the 1500 kW system was sized for an 8.1 mps (18 mph) mean wind site. Twenty one configurations were initially selected for analysis varying such parameters as rotor solidity, rotor aspect ratio, rated wind velocity, and number of rotor blades. A summary of the configurations initially studied is presented in Figure 2.

Config No.	Rated Power (kW)	Rated* Velocity mps (mph)	Number of Blades	rpm	Rotor Solidity	Rotor Aspect Ratio	Rotor Diameter meters (ft)	Rotor Span meters (ft)	Rotor Blade Chord meters (ft)
1	120	8.05 (18)	3	27.0	0.159	1.073	20.4 (67)	21.9 (71.8)	1.08 (3.5)
2	120	8.05 (18)	3	24.0	0.198	1.073	20.4 (67)	21.9 (71.8)	1.35 (4.4)
3	120	8.05 (18)	3	21.3	0.238	1.073	20.4 (67)	21.9 (71.8)	1.62 (5.3)
4	120	8.05 (18)	3	20.0	0.198	0.746	24.5 (80.3)	18.3 (59.9)	1.62 (5.3)
5	120	8.05 (18)	3	16.0	0.198	0.477	30.6 (100.4)	14.6 (47.9)	2.02 (6.6)
6	120	7.15 (16)	3	18.0	0.198	1.073	24.3 (80)	26.1 (85.6)	1.61 (5.3)
7	120	8.94 (20)	3	31.5	0.198	1.073	17.4 (57)	18.7 (61.3)	1.15 (3.8)
8	500	8.05 (18)	3	17.7	0.079	1.073	43.0 (141)	46.2 (151.5)	1.14 (3.7)
9	500	8.05 (18)	3	15.1	0.119	1.073	43.0 (141)	46.2 (151.5)	1.71 (5.6)
10	500	8.05 (18)	3	12.8	0.159	1.073	43.0 (141)	46.2 (151.5)	2.26 (7.4)
11	500	8.05 (18)	3	11.8	0.079	0.477	64.6 (211.8)	30.8 (101)	1.71 (5.6)
12	500	8.05 (18)	3	11.5	0.119	0.614	56.9 (186.6)	34.9 (114.6)	2.26 (7.4)
13	500	7.15 (16)	3	11.3	0.119	1.073	51.3 (168.2)	55.0 (180.5)	2.04 (6.7)
14	500	8.94 (20)	3	19.7	0.119	1.073	36.7 (120.5)	39.4 (129.3)	1.46 (4.8)
15	500	8.05 (18)	3	10.1	0.238	1.073	43.0 (141.2)	46.2 (151.5)	3.41 (11.2)
16	500	8.05 (18)	3	13.5	0.119	0.850	48.3 (158.6)	40.8 (134.9)	1.92 (6.29)
17	1,500	11.60 (26)	3	18.5	0.159	1.073	43.0 (141.2)	46.2 (151.5)	2.26 (7.4)
18	1,500	11.60 (26)	3	14.6	0.238	1.073	43.0 (141.2)	46.2 (151.5)	3.41 (11.2)
19	1,500	11.60 (26)	3	12.7	0.317	1.073	43.0 (141.2)	46.2 (151.5)	(4.54) (14.9)
20	1,500	11.60 (26)	4	14.2	0.238	1.073	43.0 (141.2)	46.2 (151.5)	(2.56) (8.4)
21	1,500	11.60 (26)	5	14.6	0.238	1.073	43.0 (141.2)	46.2 (151.5)	2.04 (6.7)

*Wind velocity specified at a height of 9 meters; uprated to 30 meters for Giromill power definition.

GP77-0007-36

FIGURE 2
GIROMILL STUDY CONFIGURATIONS

2.2 Optimum Giromill Design

Cost analysis of the 21 configurations evaluated indicated that a 1500 kW system would have the lowest energy cost. This low cost, however, was almost entirely due to the ground rules that these large systems be placed in a high (8.1 mps) mean wind. Only a few sites with this high mean wind are available.

To make a Giromill cost optimization effort more meaningful, it was decided that a 500 kW unit placed in a 5.4 mps mean wind would be optimized. Giromill configuration No. 11, which had the lowest energy cost, was selected for this optimization effort.

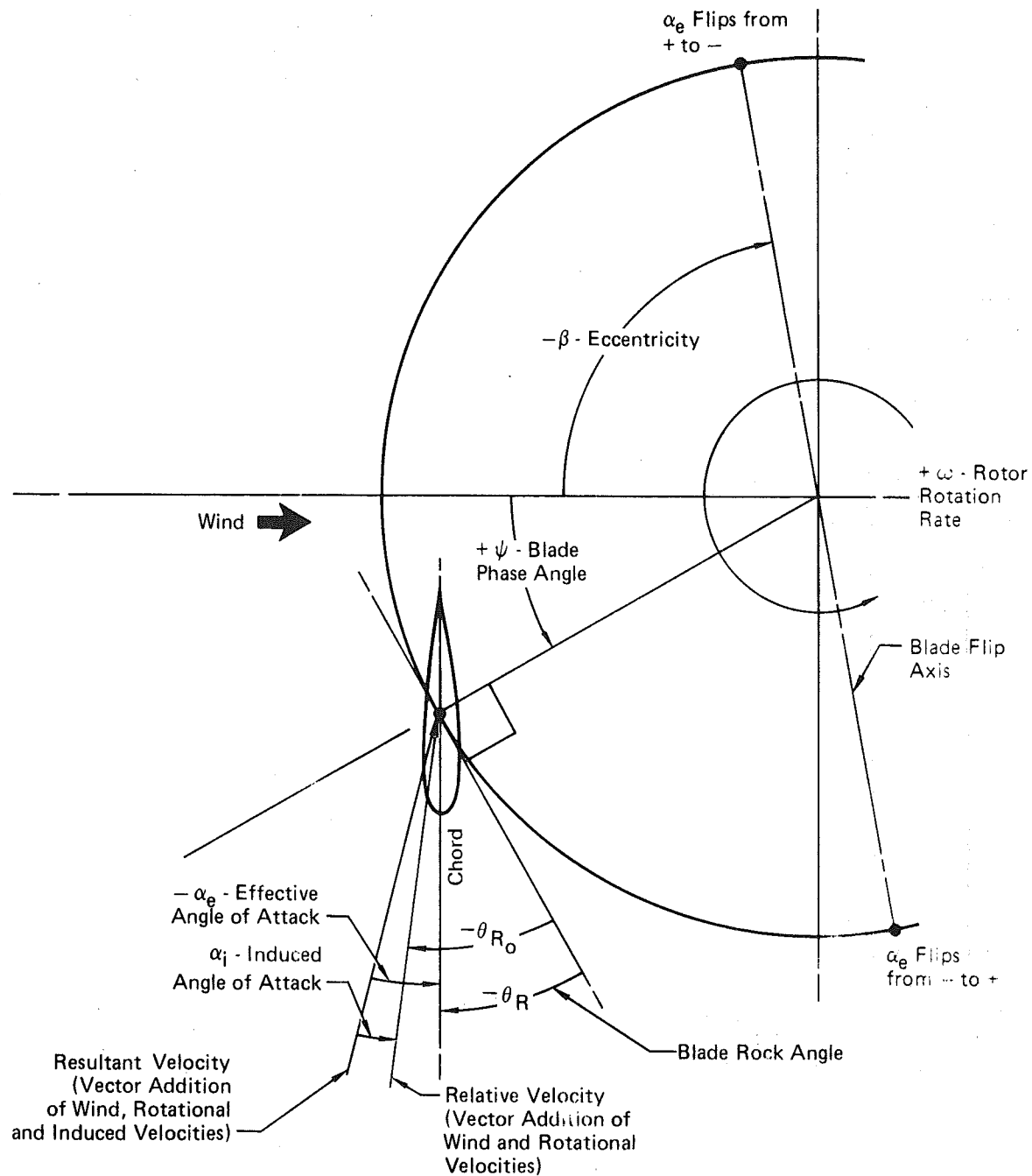
3. AERODYNAMICS AND PERFORMANCE

3.1 Aerodynamic Analysis

The fundamental problem in determining the Giromill performance is finding the magnitude and direction of the local velocity at all points on the blade orbit so that the blade forces can be computed. The vortex theory computer program requires the two-dimensional wing section lift and drag characteristics. Two dimensional or section aerodynamic characteristics are required for running the program since the local resultant velocity of the wind, consisting of the vector addition of the wind, blade orbit rotation velocity, and calculated induced velocities, is used for computing the forces on the blades. The blade aerodynamic characteristics are presented in terms of an effective angle of attack, α_e , which is the same as the section angle of attack, and is measured from the resultant velocity to the blade chord. Figure 3 defines the various angles and other rotor relations used throughout the report.

The aerodynamic characteristics previously used in the mid-term report were for the NACA 0015 and NACA 64₂015 airfoils. In the course of improving the Giromill system, it was found that a thicker blade section decreased in structural weight faster than the drag increased providing a more cost effective system. It was also determined that an airfoil having a gradual stall characteristic was also desirable. This lead to selection of the NACA 64₄021 airfoil for the optimized system. Reference 2 gives the aerodynamic characteristics up to stall for NACA 64₄-021; they vary of course, with operating Reynolds number. The effective Reynolds number (R_N) at the Giromill blade varies with position on the blade orbit. On the side where the blade is moving upwind the Reynolds number is greater than on the downwind side. For the optimum design Giromill configuration 11-1 (see Section 4) at an operating blade speed ratio of 3.85, the upwind R_N is 4.4×10^6 , and the downwind R_N is 2.6×10^6 . An average R_N of 3×10^6 was therefore used for the performance analysis. The aerodynamic characteristics used are shown in Figures 4 and 5. When computing the blade loads for structural strength analyses the aerodynamic characteristics for a R_N of 9×10^6 were used which increased the max C_ℓ to 1.45 at an α_e of 22 deg. This is because the blade R_N can reach 6.6×10^6 under wind gusting conditions, and the higher C_ℓ at the higher R_N should be accounted for in the structural analysis.

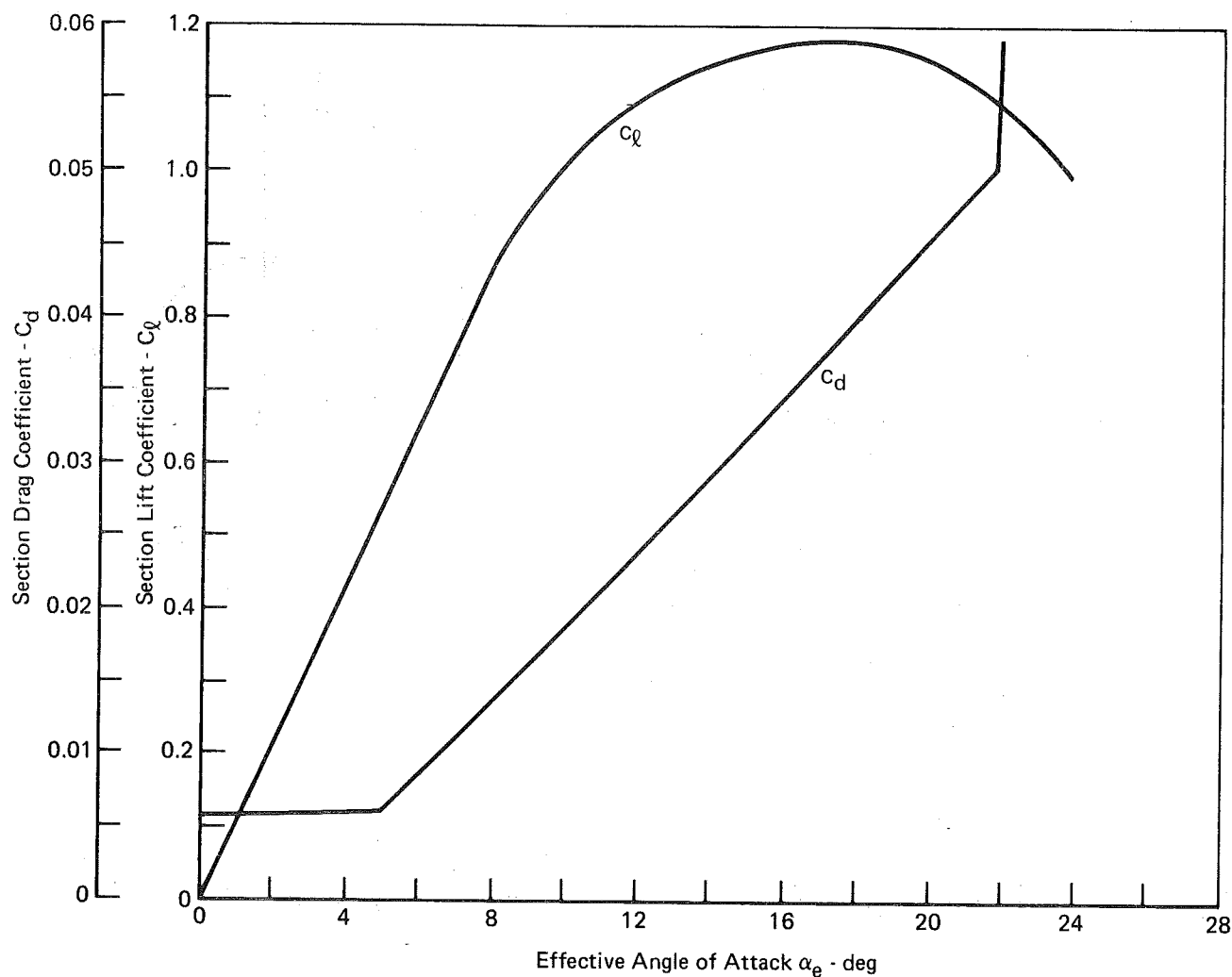
The vortex theory program employed was developed by Prof. H. C. Larsen from the Air Force Institute of Technology and was fully explained in Reference 1. Briefly, this theory assumes that a series of free vortex rings are generated



Note: Some angles shown negative to be consistent with normal Giromill operating conditions.

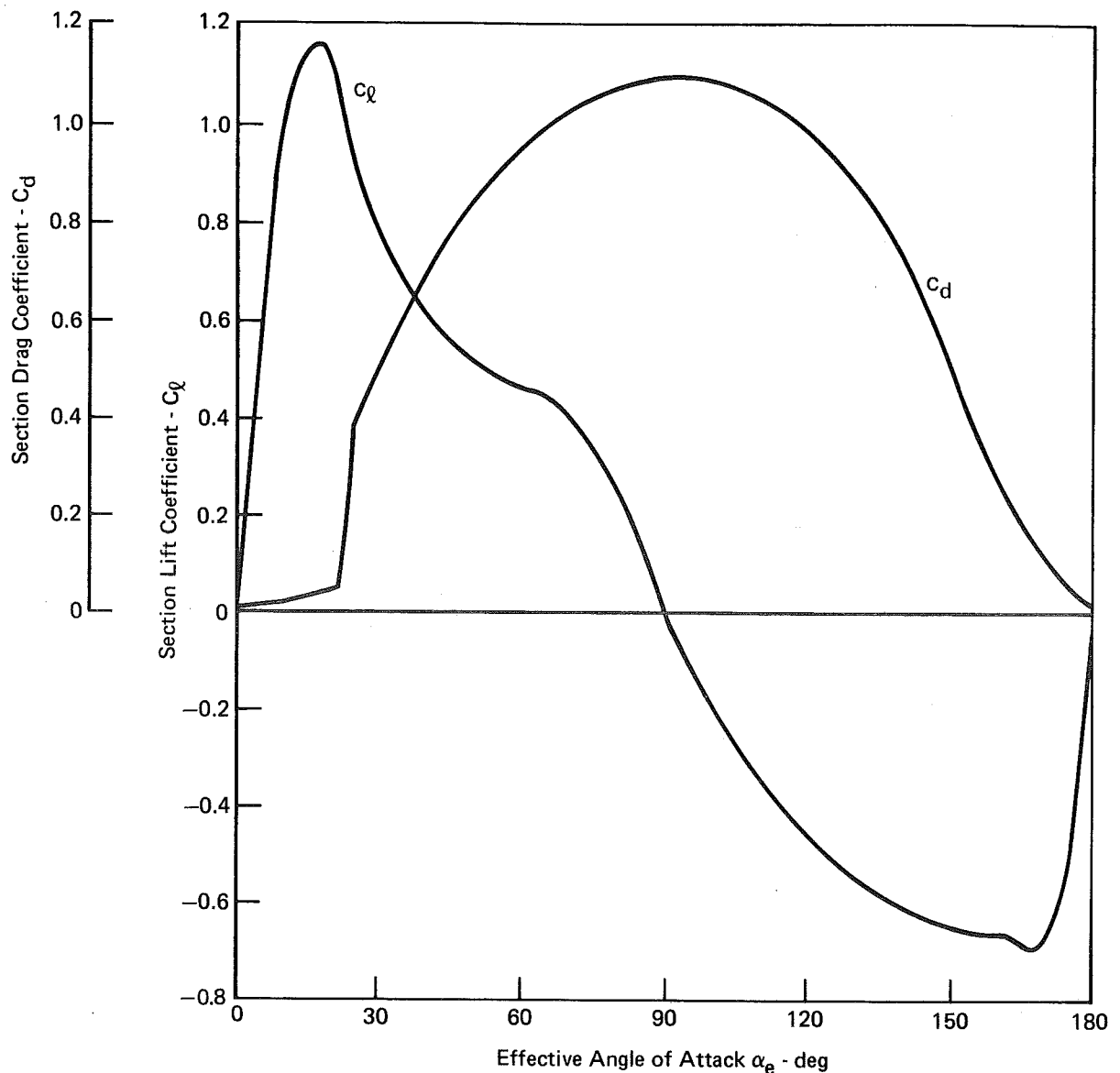
GP77-0007-1

FIGURE 3
CYCLOGIRO ROTOR PARAMETERS DEFINITION



GP77-0007-2

FIGURE 4
TWO-DIMENSIONAL (SECTION) AERODYNAMIC CHARACTERISTICS USED
FOR PERFORMANCE CALCULATIONS
 Low α_e



GP77-0007-3

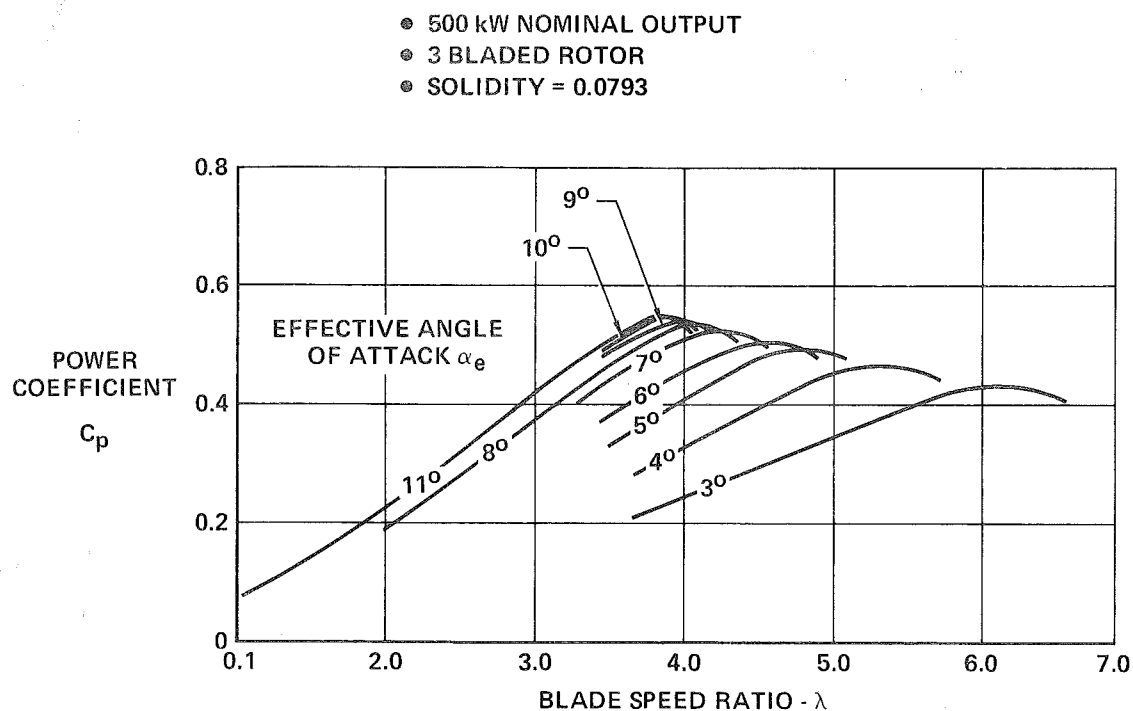
FIGURE 5
AIRFOIL SECTION CHARACTERISTICS USED FOR
PERFORMANCE CALCULATIONS
 Through $180^\circ\alpha_e$

by the alternate flipping of the blades from a positive to a negative and then back to a positive angle of attack as the blade follows an orbit around the rotor. These vortices are carried downstream with the fluid. The induced effects of these vortices and the bound vortices are computed and the blade attitude (rock angle) set to establish the commanded effective angle of attack α_e . An iteration scheme is employed and a solution is obtained when the momentum flux through the capture area induced by the vortices agrees with the momentum flux calculated from the forces on the blades.

This theory is only applicable for a vertical axis system that has articulating blades. It cannot be used to compute the performance of a Darrieus type rotor.

3.2 Performance

Figure 6 presents the Giromill performance characteristics for the optimized 500 kW system. These power coefficient, C_p , characteristics were determined using the NACA 64₄021 airfoil characteristics at R_N of 3×10^6 . They were computed using the cyclogiro vortex theory computer program. The maximum C_p is seen to occur at a blade speed ratio, λ , of 3.85 at an α_e of 11° .



GP77-0007-53

FIGURE 6
GIROMILL PERFORMANCE CHARACTERISTICS

Figure 7 compares these final report characteristics with those obtained in our mid-term report, and shows that these revised characteristics exhibited a flatter trend with λ . The reason for this flatter trend was found to be caused by the lower solidity, σ . The mid-term Giromill performance was based on a solidity, σ , (based on capture area - span times diameter) of 0.198. The revised curves have a solidity of 0.079. The beneficial result of this flatter trend is to increase the yearly power output. This is discussed in Section 7.2.

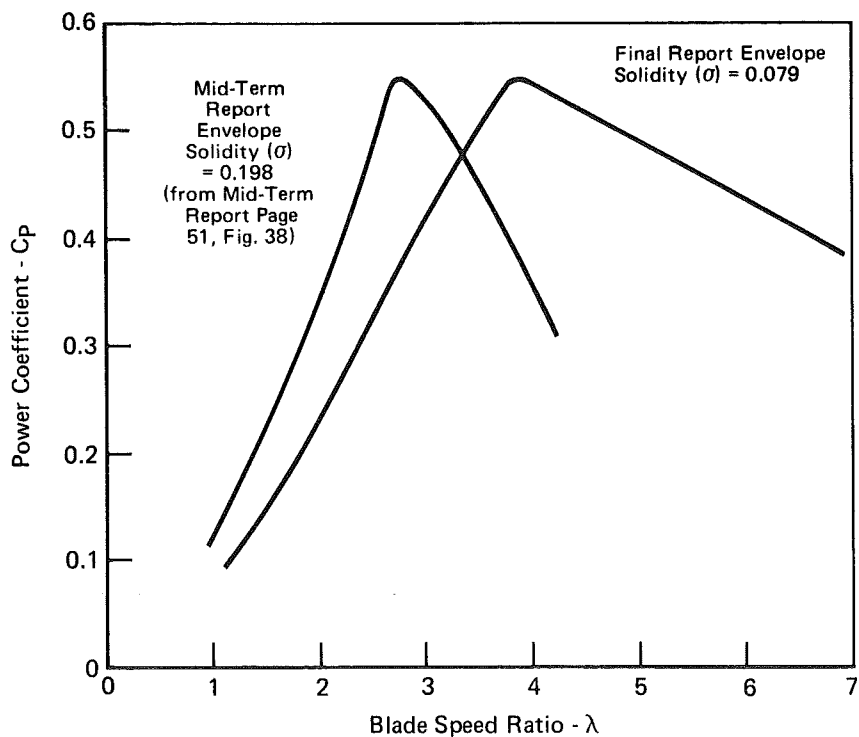


FIGURE 7
PERFORMANCE ENVELOPE COMPARISON

Cross plotting the effective angle of attack, α_e , that provides the $C_{p_{\max}}$ in low wind region (high λ) from Figure 6, results in the curve of Figure 8. Setting the Giromill operating point so that max C_p is achieved at a $V_R = 8.1$ mps, results in the $C_{p_{\max}}$ and α_e characteristics with V_W as shown in Figure 9.

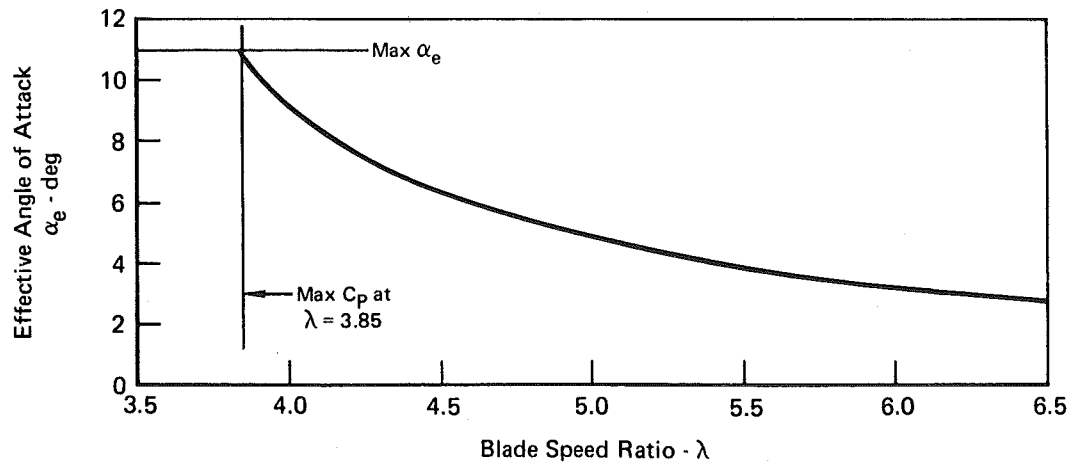
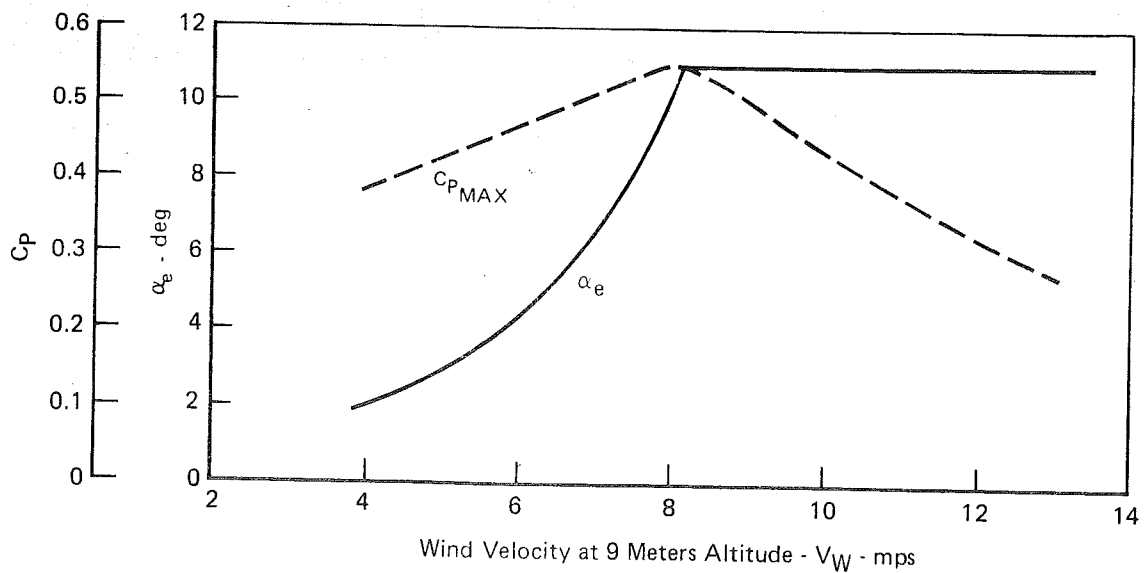


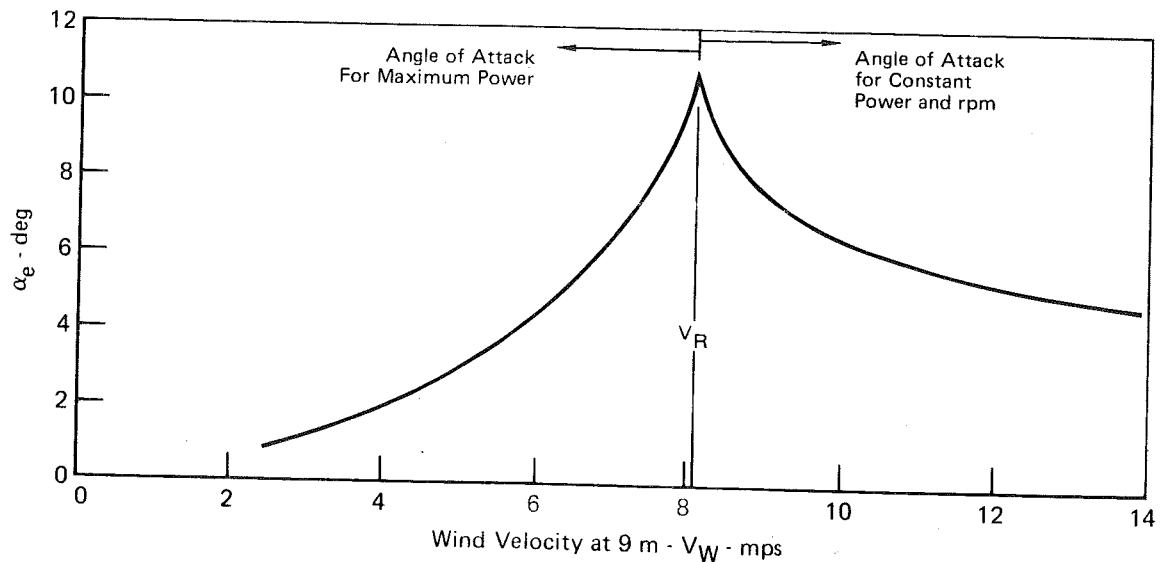
FIGURE 8
 α_e FOR $C_{P_{\max}}$ AT HIGH λ



GP77-0007-6

FIGURE 9
 $C_{P\text{MAX}}$ AND CORRESPONDING α_e

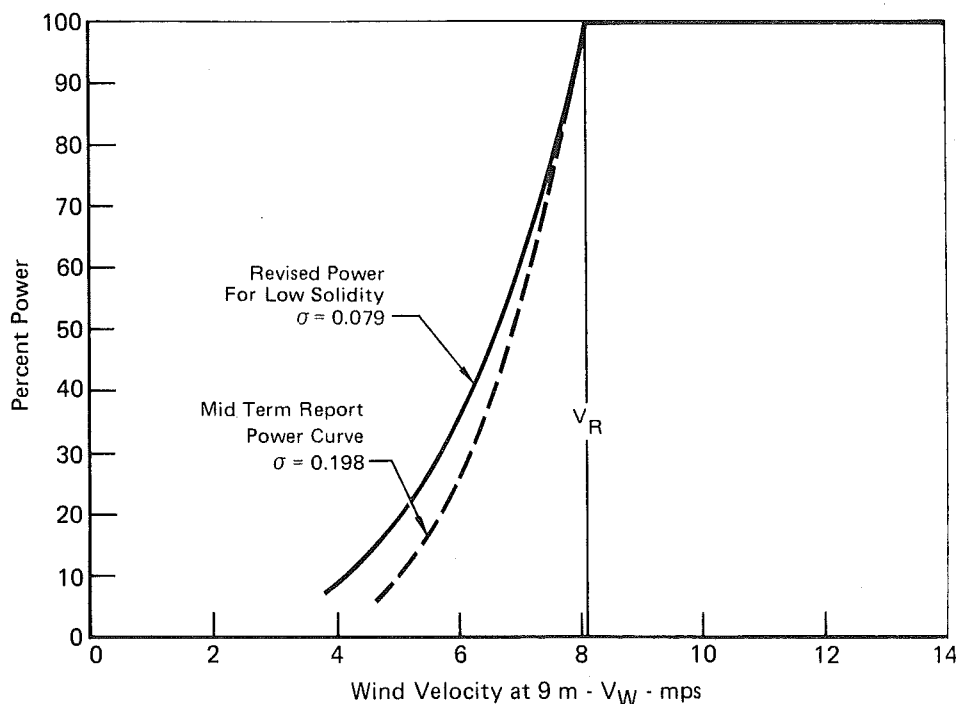
The Giromill is operated so that in the low wind region ($V_W < V_R$), the blades are modulated to provide the maximum power. The α_e curve of Figure 9 for $V_W < 8.1$ mps is therefore the desired α_e profile. For $V_W > 8.1$ mps, the blades must be modulated at a reduced α_e to provide for a constant power and rotor RPM. The α_e to implement this has been determined and is shown in Figure 10.



GP77-0007-7

FIGURE 10
ANGLE OF ATTACK PROFILE

The resulting power curve using the α_e profile from Figure 10 is shown in Figure 11 along with the power curve we obtained in our mid-term report. The increased power output at the low wind velocities because of the flatter C_p curve due to a lower σ results in a 3% increase in yearly power generated. Section 7.2 discusses this further.



GP77-0007-8

FIGURE 11
GIROMILL POWER

Other Giromill performance features that were discussed in our mid-term report and were determined using the Larsen cyclogiro vortex theory computer program are summarized below:

- (1) Power output was found to be independent of rotor aspect ratio.
- (2) Power is proportional to the rotor capture area (rotor diameter times span).
- (3) Design RPM varies inversely with rotor diameter. For a given power, therefore, a high rotor aspect ratio system will have a higher RPM than a low rotor aspect ratio.
- (4) Design RPM varies inversely with solidity.
- (5) Maximum efficiency is independent of number of blades and solidity.
- (6) For a given power and solidity system, design RPM varies directly with rated wind speed.

4. GIROMILL SYSTEM DESIGN

The Giromill baseline design approach was to investigate a concept that would be adaptable with minimum modifications to the complete kW range analyzed. This led to a design concept having the blades supported on tubular radial arms attached to a triangular central tower. Diagonal tension members support the main radial arm to which the blade rock actuator is attached. The other radial arms are stabilized through the blades. The central (or upper) tower is cantilevered from the lower tower by an upper main rotor bearing mounted on a bulkhead on the lower base tower, to another main bearing also mounted on the lower tower just above the RPM speed increaser. This provides the maximum couple distance between bearings. The upper and lower towers are constructed from structural steel members bolted together. A standard RPM speed increaser and generator are ground mounted for easy accessibility. A sketch of this concept is shown in Figure 12.

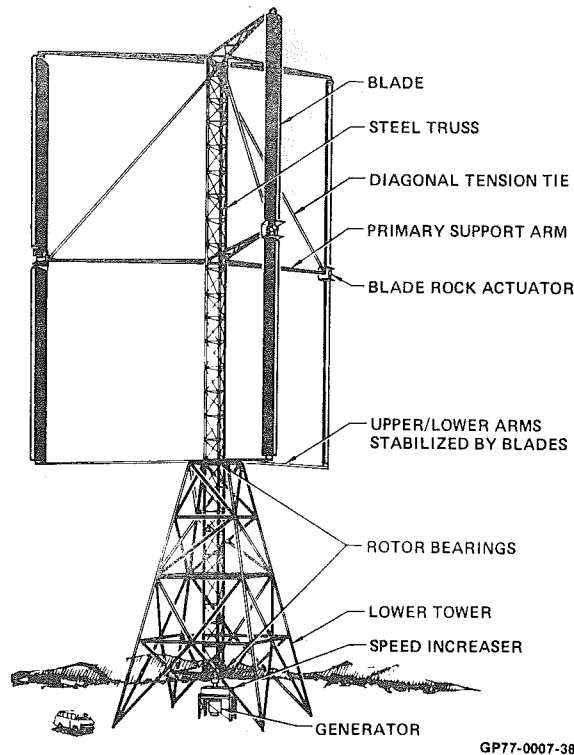
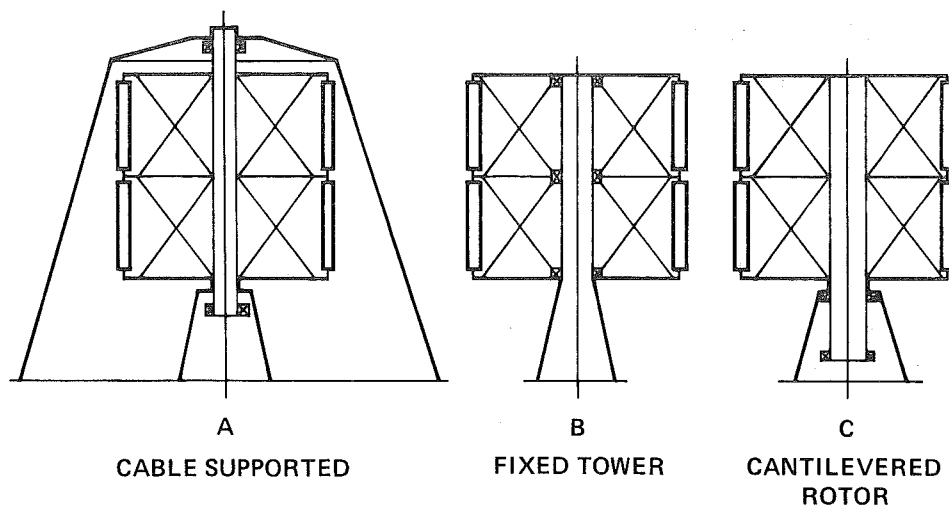


FIGURE 12
GIROMILL CONFIGURATION

This cantilevered design was determined to be the best over a cable supported and fixed tower concept studied and shown in Figure 13. The cable supported rotor (A) had an upper and lower bearing. The upper bearing was above the rotor and was supported by a spider truss supported by cables. The structu-

ral dynamics due to the cable sag and sway, the increased load in the lower bearing due to cable tension, the requirement for the large stiff spider cable support arms, and the large area of real estate required for the cable tie down were the negative aspects of this type of design. The fixed tower design shown in (B) appeared attractive except for providing a power drive to the generator. There appeared to be no cost effective method of transmitting the rotor torque to a generator drive shaft. Using a single ring and pinion gear at the bottom or middle blade support requires that the entire rotor torque be directed through that gear. This requires a heavy blade support structure. Three ring gears (one at each blade support) could be used, however, the mechanical complexity and the long drive shaft are the negative aspects. Concept (C) was the design selected for this feasibility study, and consists of a simple structural built-up rotating upper tower cantilevered from the lower stationary tower.



GP77-0007-39

FIGURE 13
CONCEPTUAL DESIGNS INVESTIGATED

The initial analysis of the 21 Giromill configurations, previously listed in Figure 2, showed that the 500 kW systems had a lower energy cost than the 120 kW systems when they were placed in the same mean wind (5.4 mps) environment. (See Section 8.3 for an energy cost summary.) The 1500 kW systems had a still lower energy cost, however, this can be attributed almost entirely to the higher mean wind (8.1 mps) environment that these systems were designed for. Since there are only a few areas where a mean wind to 8.1 mps exists, it was decided to concentrate the Giromill optimization effort on a 500 kW system to be installed in a 5.4 mps mean wind.

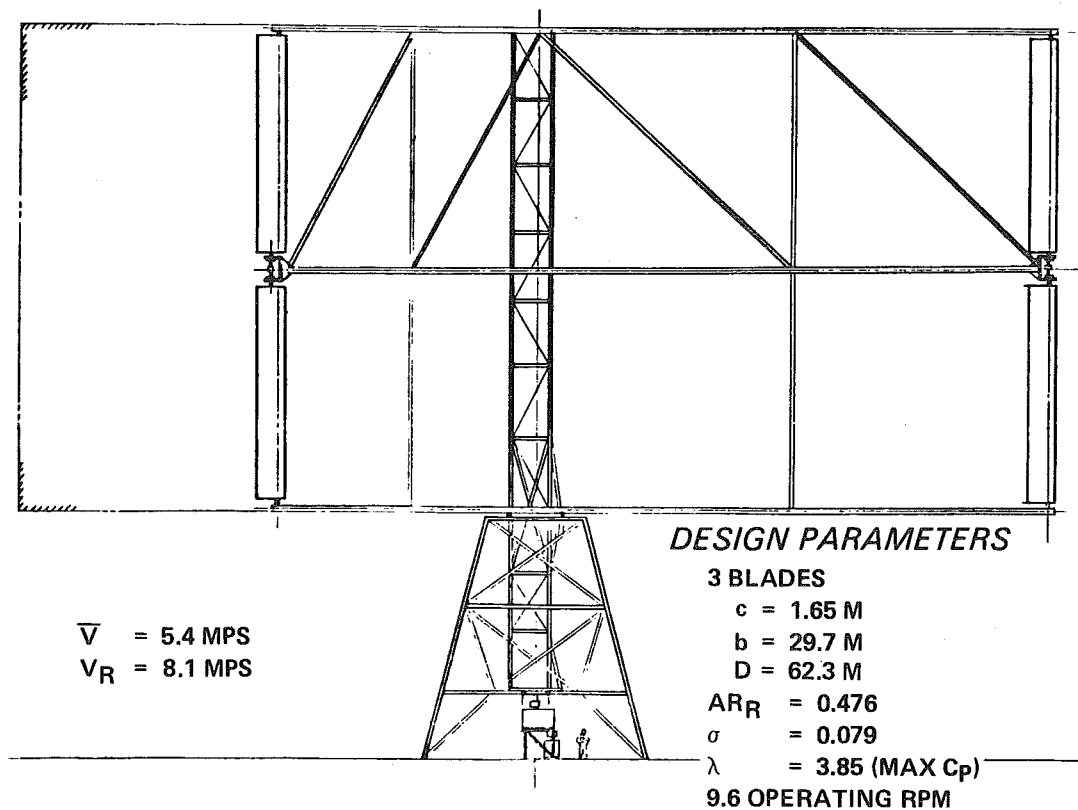
The cost analysis indicated that a low rotor aspect ratio Giromill was more cost effective. For example, compare the energy cost between configurations 8 and 11 shown in Figure 42 on page 56. This is because of the smaller main bearings required for the lower rotor aspect ratio configurations. In fact, configuration 11, which had a rotor aspect ratio of 0.477, resulted in the least energy cost for Giromills placed in a 12 MPH (5.4 mps) mean wind site and was selected for the optimization effort.

The optimization effort included the following changes from our mid-term design:

- (1) The blade section aerodynamics for an NACA 64₄021 airfoil were used instead of a NACA 64₂015. The performance was based on the smooth surface characteristics at a Reynolds number of 3×10^6 . For conservatism the blade loads were based on the characteristics at a Reynolds number of 9×10^6 .
- (2) A 120 MPH (54 mps) constant high wind condition was assumed. No wind velocity height uprating was incorporated for this condition. This allowed a more optimum structural design since the service life and ultimate load criteria were compatible. Appendix A discusses the ramification of this ground rule.
- (3) The lower main bearing was reduced to 1.5 meters instead of having to extend around the tower diameter as was assumed in our mid-term report. This was possible since it did not affect the upper tower structural rigidity or dynamics.
- (4) The lower main bearing instead of the upper was designed to take the tower weight. The upper main bearing now just has to react the tower moment. It is felt this would result in a lower cost upper bearing, however, no cost reduction was incorporated in the cost analysis.

The results of applying these changes and performing the analyses resulted in the configuration shown in Figure 14. This configuration is denoted as configuration 11-1.

The size was slightly reduced from the initial configuration 11 because of the effect of the 64₄021 smooth aerodynamic characteristics. The diameter was reduced from 64.6 meters to 62.3, and the blade span from 30.8 to 29.7 meters.



GP77-0007-41

FIGURE 14
500 kw GIROMILL CONFIGURATION 11-1

Only three blade support arms, instead of four, were used. This increased the blade weight but overall provided a lighter designed system. This also reduced the blade actuator costs since it was determined that a single actuator mounted on the center support arm was sufficient for each blade. The mid-term report had assumed two actuators per blade.

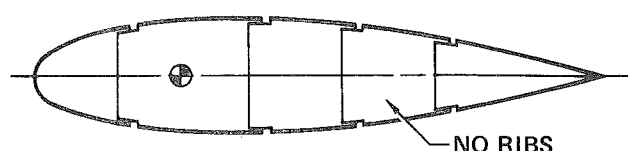
Reducing the high wind ground rule and optimizing the structure resulted in a reduction of the central tower diameter from 3.75 meters to 2.62 meters with a corresponding reduction in main bearing size. As previously noted, this reduced wind was the cross over wind between fatigue design of the tower and high wind load bending design.

All other design features that were incorporated in our mid-term design were retained.

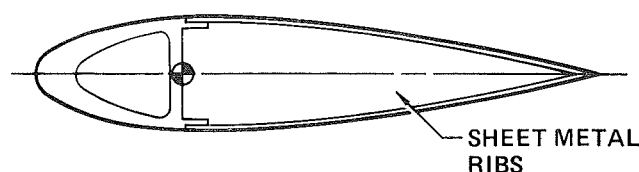
The blades are constructed of a rolled aluminum leading edge and brake formed spar backed by a thin beaded aluminum sheet metal trailing edge stabilized by ribs. This type of blade construction was found to be the most cost effective of the blade concepts investigated and shown in Figure 15. Concept (A) had initially shown promise because of its ease of manufacture since it had no ribs.

It had, however, a relatively high polar moment of inertia and required considerable ballast to locate the CG at the pivot point (25% chord). Concept (B) had an extruded leading edge torque box with a sheet trailing edge stabilized by sheet metal ribs fastened to the leading edge extrusion. It was found that a closed "D" type extrusion as shown was expensive and not very practical. Two extrusions, a leading edge and a spar in place of the "D" extrusion was also evaluated, but was still not as attractive as concept (C). Because the blades are symmetrical and have a constant chord they lend themselves to the rolling and brake forming of the leading edge and spar, and constructing as shown in (C).

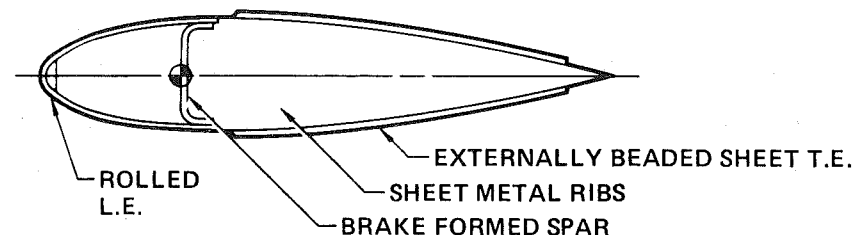
(A) ROLL FORM/WELD BOND



(B) EXTRUDED L.E. SHEET T.E.



(C) FINAL CONFIGURATION



BASELINE REQUIREMENTS

- 1 INEXPENSIVE
- 2 C.G. AT PIVOT POINT (25% CHORD)
- 3 LOW POLAR MOMENT OF INERTIA TO MINIMIZE ROCK ANGLE ACTUATOR

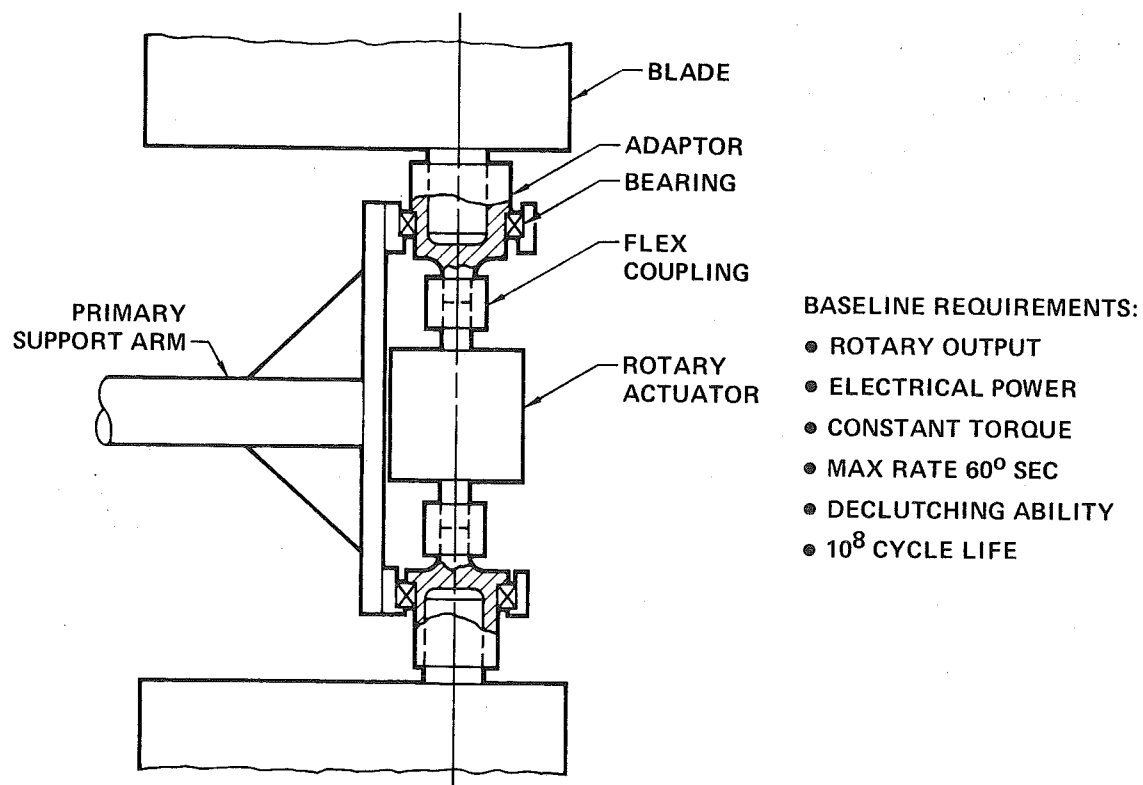
FIGURE 15
BLADE CONCEPTS INVESTIGATED

A standard type of speed increaser coupled to an a.c. synchronous generator was employed. This is the same concept as evaluated by G.E. and Kaman for the conventional type of windmill. The Giromill system would have the same type of operating characteristics as a conventional windmill and hence the electrical utility hook up and operating features would be similar.

The blade rock angle actuator concept employed is shown in Figure 16. The rotary actuator is a brushless DC motor driving through an electrical clutch to a speed reducer to the blade. The critical life cycle component was determined

GP77-0007-40

to be the bearings. The 120 kW systems required an actuator having a maximum power output of 0.6 HP; the 500 kW required 5 HP, and the 1500 kW 15 HP.



GP77-0007-42

FIGURE 16
BLADE ROCK ANGLE ACTUATOR

5. STRUCTURAL/STRENGTH DESIGN

The structural arrangement of the Giromill was studied as three sub-structures: 1) blades, 2) blade supports, and 3) tower. Each of these sub-structures were sized using the following structural design criteria:

- 1) Service Life - Dynamic components, e.g., blades, shall endure the loads spectrum associated with a 30 year service life. Static components, e.g., lower tower, shall endure the loads spectrum associated with a 50 year service life.
- 2) Structural Dynamics - Dynamic resonance at rated operating conditions shall be avoided. Blade flutter and mechanical instabilities shall not occur under any operating conditions.
- 3) Ultimate Loads - Ultimate loads equal the factor of safety times the maximum expected loads. A factor of safety of two shall be used for blade design, and a factor of safety of three shall be used for blade support and tower design. The structure shall sustain ultimate loads without failure.

Three loading conditions were used in sizing the Giromill structure. These are as follows:

- 1) Normal operation under rated conditions
- 2) Operation under wind gust conditions
- 3) High winds

5.1 Structural Arrangement

Low-drag, three-bladed rotors and a clean straightforward design characterize the structural arrangement of the Giromill as portrayed in Figure 12. Three blades were selected over two, four, etc., to preserve polar symmetry while minimizing the blade support structure required.

Giromill blades exhibit a constant cross section and stiffness along their length. Airfoil thickness is 20% of chord. The leading edge skin and single spar (main box) carry all spanwise loads. The trailing edge is corrugated chordwise and provides both a load path to the main box and torsional stiffness. Main ribs distribute loads at blade supports, and secondary ribs are spaced throughout the blade for minor load redistribution and stiffness. Blades are ballasted to locate the center of gravity at the centerline of blade rotation, 25% chord. Close tolerance mechanical fasteners are used for assembly.

Blade loads for operating conditions consist of airloads, which are radial and tangential with respect to the blade orbit, and centrifugal loads.

Radial and tangential load supports are provided for each blade at three or more places in the Giromill systems studied. Blades are supported torsionally and vertically at the center support. In high winds, blades are declutched and allowed to weather vane into the wind.

Radial and tangential load supports for each blade consist of planar trusses (frames) each extending radially from the tower to an apex at the blade. Each frame consists of two columns joined by a blade attach fitting at the apex and cross-braced for increased in-plane strength and stiffness. Three or more blade supports are generally required to maintain acceptable blade stress levels. A tension brace extends diagonally from the top of the tower to the blade. It provides the necessary load path for vertical loads. Combination (thrust) bearings are used at all blade/support interfaces, so unbraced frames are supported vertically by the blade. Large radius rotors require additional out-of-plane frame bracing to preclude structural instability.

The Giromill tower is composed of an upper and lower section. The upper tower rotates as a part of the rotor and effectively forms a torque shaft connecting the torque-generating blades to the speed increaser and generator at the base of the tower. To reduce wind loading, the upper tower is designed as an open lattice structure which has a triangular cross section. Corner posts are columns designed for the combination of dead weight and overall tower bending, which results from blade loads and wind loads on the structure. Cross bracing between the corner posts provides the necessary column stability.

The diagonals in each of the three tower faces are also designed as columns capable of sustaining 100% of the shear loads on the tower. Diagonals and corner posts considered together provide the flexural and torsional stiffnesses necessary to preclude strong resonances with the primary dynamic excitations.

Bulkheads housing large diameter bearings are located in the upper tower and in the lower tower at each end of the upper/lower tower overlap. Initially the upper bulkheads were designed for lateral (tower shear) and vertical (structural weight) loads while the lower bulkheads were designed for lateral loads only. It was later found more cost effective to have the lower bulkhead support the tower weight. In addition to facilitating load transfer between the upper and lower tower sections, a long overlap increases the tower torsional stiffness by reducing the length of the actual torque shaft connecting the rotor to the ground-based power generating equipment.

The lower tower section is an open lattice structure designed to the same criteria as the upper tower but rectangular in cross section. The batter (slope of the corner posts) of this section can be adjusted to provide the necessary base rigidity. A steel grillage foundation or cast-in-place pier-with-bell anchors each cornerpost.

5.2 Structural Design

For a Giromill operating at rated power and under rated wind and rotor speeds, the variation in operating loads as the rotor makes one revolution was used to define the fatigue environment. In this feasibility study, the effects of resonance dwell during start up and shut down and the effects of operating at wind speeds other than rated speed were not considered. Also, the beneficial effects of occasional high load cycles from wind gusts were ignored. The relatively high load cycles associated with the wind gust condition occur too infrequently to cause fatigue damage.

Based on this variation in normal operating loads and the service life requirements, 10^8 to 10^9 load cycles can be expected in any structural member. For most engineering materials, this means operating at stress levels at or below the material's constant amplitude, fatigue endurance limit. The combination of infinite life, load cycle characteristics, and structural configuration defines this allowable stress (endurance limit) for the selected material. Because of the large number of load cycles which accrue in a year, the allowable stress for a service life of one year will be only slightly higher than that for a service life of 30 years.

A design ultimate load is equal to the maximum expected load times a factor of safety (F.S.). For blade design, a F.S. of 2 is consistent with the materials and manufacturing quality associated with aerospace structures. To maintain low operating stress levels in blade support and tower structure, a F.S. of 3 is used. This factor is characteristic of commercially constructed transmission towers and buildings. Structural stability considerations dictate allowable stress levels for design ultimate loads.

In this study, the high wind and gust wind loadings comprise ultimate load conditions. Blades are declutched and allowed to weather vane during high winds; however, wind loads in conjunction with a reasonable structural solidity does become a design consideration for the tower.

Ultimate gust loads are accounted for in the blade design only. A gust which is sustained long enough to load the entire Giromill structure would precipitate either a blade declutching because the cut-off wind speed is reached

or change the blade modulation to counter the increased wind speed. In either case, blade loads and thus total tower loads are reduced.

5.2.1 Blade Design - The design of Giromill blades is basically dictated by service life requirements. As such, the peak loads associated with normal operation under rated conditions become the design loads. Gust loads become important in low aspect ratio, large blade chord systems where large flat-plate areas of the leading edge are stability critical rather than fatigue critical.

Air and inertia loads resolved along the chord were found to be small relative to the loads acting normal to the blade chord and are not included in the blade analysis. The constant inertial loads plus the variable air loads produce a one per revolution load cycle. For the 120 kW system, inertial loads are high relative to airloads. The lower rotor speed of the 500 and 1500 kW systems results in minor blade load reversal under normal operation. For all systems a load or stress ratio of zero (minimum load divided by maximum load) is used in determining an allowable stress for the fatigue loading.

An aluminum alloy was selected for the blade material. In addition to the high structural efficiency of aluminum relative to other common materials, such as steel, aluminum is easily formed, naturally resistant to galvanic corrosion and the selected alloy, 2024-T6, exhibits good resistance to stress corrosion. All of these factors are considered important, for maintenance reasons, to the design of a long-life, closed structure.

The endurance limit of this aluminum, for a stress ratio of zero and a stress concentration factor representing spanwise patterns of mechanical fasteners, is 96.5 MN/m^2 (14000 psi).

5.2.2 Blade Supports and Tower Design - The blade supports and tower are the major weight items of the Giromill system. Because of the expected impact of these substructures on total system costs, materials and fabrication techniques used commercially for structures such as transmission towers are relied upon as representing the maximum economy possible in this type of construction. Consequently, commercial steels, such as A-36, A-441, and A-514, were selected for the blade support and tower substructures. The factor of safety of 3 chosen for this analysis effects maximum expected stresses approximately equal to those specified by agencies governing the design of commercial structures, such as the AISC. Load associated with high wind condition and normal operation must both be considered.

For normal operation of three-bladed rotors, tower loads repeat every 120° of rotor travel yielding three load cycles per revolution. A comparison of the various Giromill systems indicates that peak tower loads are proportional to the rated power of the system.

5.3 Structural Sizing Results

The sizing results for the three sub-structures for the Giromill configurations analyzed is shown in Figure 17. All of these configurations reflect the same design criteria and analytical methods. A late addition to the matrix of configurations, Configuration #16, was eventually judged unnecessary and the sizing and cost analyses were not completed.

5.4 Configuration 11-1 Structural Analysis

Configuration 11 was selected for further analytical refinement because it showed the lowest energy cost for the 500 kW systems. Aerodynamic and structural analyses were refined to further enhance the cost effectiveness of this configuration, which is now referred to as Configuration 11-1.

A significant weight savings is realized by 1) beefing up the blades such that fewer blade supports are required, and 2) using a constant 54 m/sec (120 mph) wind for the high wind load condition.

For the operating condition, limit blade and tower loads are presented in Figures 18 and 19 for Configuration 11-1. These loads are slightly conservative in that high Reynolds number aerodynamic characteristics were used for airload calculations. Constant amplitude endurance limits for 2024-T6 aluminum (blade material) and commercial grades of carbon steel (blade supports and tower material) were used as allowable stresses for service life design requirements. It is important to note that load amplifications which occur while passing through primary resonances during startup and shutdown have not been considered in this analysis.

Previously, the blade supports and tower structure designs were dictated entirely by the ultimate load criterion. Due to the change in average wind speed for the high wind condition, the designs of these items are now dictated by both the service life and ultimate load criteria. The blade supports and tower substructures are still basically compression structures sized to ultimate loads from the storm wind condition; however, members designed to these loads, in general, exhibit limit (expected) operating stresses which exceed fatigue allowables at member splices. For Configuration 11-1, these joints were beefed up to reduce operating stresses to an acceptable level.

Configuration	AR/R	Span (Ft)	Radius (Ft)	Chord (Ft)	Number of Blades	V _R (mph)	ω (rpm)	Tower Dia (Ft)	No. of Blade Support Arm	Blade Weights (Lb)	Blade Support Weights (Lb)	Upper Tower Weight (Lb)	Lower Tower Weight (Lb)	Total Tower Weight (Lb)	Total System Weight (Lb)
120 kW	1	1.073	71.85	33.48	3.54	3	18	5.02	3	5,430	8,220	19,280	18,050	37,330	50,980
	2	1.073	71.85	33.48	4.43	3	18	5.02	3	4,230	8,330	19,280	18,050	37,330	49,480
	3	1.073	71.85	33.48	5.31	3	18	5.02	3	4,750	8,390	19,280	18,050	37,330	50,470
	4	0.746	59.9	40.175	5.31	3	18	4.19	3	3,950	12,430	14,220	16,800	31,020	47,400
	5	0.477	47.9	50.2	6.64	3	18	3.35	3	3,950	21,050	10,830	16,450	27,280	52,280
	6	1.073	85.6	39.9	5.28	3	16	5.98	3	5,830	13,190	29,300	21,050	50,350	69,370
	7	1.073	61.33	28.55	3.78	3	20	4.29	3	3,200	5,500	13,390	15,950	29,340	38,040
500 kW	8	1.073	151.5	70.6	3.73	3	18	18.5	5	13,950	38,780	90,790	36,700	127,490	180,230
	9	1.073	151.5	70.6	5.6	3	18	18.5	4	16,960	37,060	98,000	36,800	134,800	188,820
	10	1.073	151.5	70.6	7.4	3	18	18.5	4	14,800	36,970	98,000	36,800	134,800	186,570
	11	0.477	101	105.9	5.6	3	18	12.3	4	7,350	79,100	43,180	26,750	69,930	156,380
	12	0.614	114.6	93.3	7.4	3	18	14	4	10,930	60,760	54,350	29,200	83,550	155,240
	13	1.073	180.5	84.1	6.7	3	16	22	4	19,330	58,750	154,480	46,200	200,680	278,760
	14	1.073	129.3	60.25	4.8	3	20	15.8	4	15,730	24,060	65,540	30,400	95,840	135,630
	15	1.073	151.5	70.6	11.2	3	18	18.5	3	21,280	45,260	117,370	37,950	155,320	221,860
	16														
1500 kW	17	1.073	151.5	70.6	7.4	3	25.95	18.5	5	15,460	46,210	91,700	36,990	128,690	120,360
	18	1.073	151.5	70.6	11.2	3	25.95	18.5	4	24,300	60,350	99,380	37,210	136,590	221,240
	19	1.073	151.5	70.6	14.9	3	25.95	18.5	4	32,330	65,600	100,280	37,490	137,770	235,700
	20	1.073	151.5	70.6	8.4	4	25.95	18.5	4	23,830	78,400	101,260	37,780	139,040	241,270
	21	1.073	151.5	70.6	6.7	5	25.95	18.5	4	28,190	95,930	100,500	37,540	138,040	262,160

GP77-0007-37

FIGURE 17
GIROMILL GEOMETRIC DATA AND DESIGN WEIGHTS

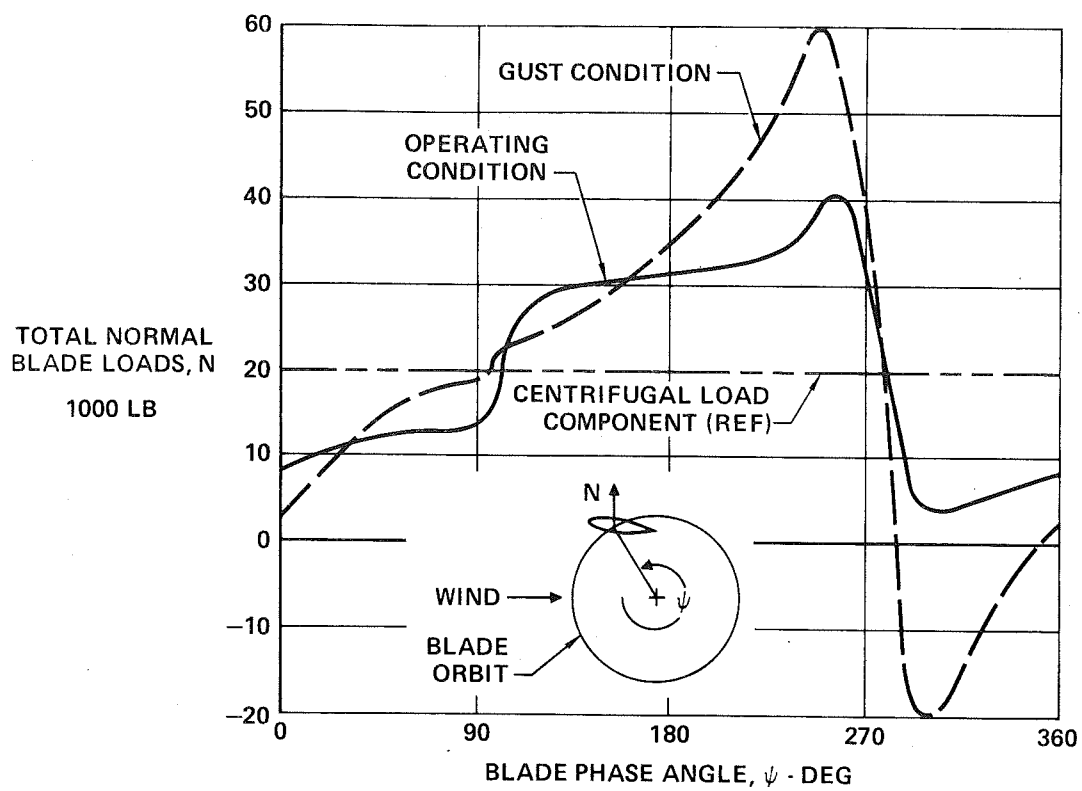


FIGURE 18
BLADE LIMIT LOADS

GP77-0007-43

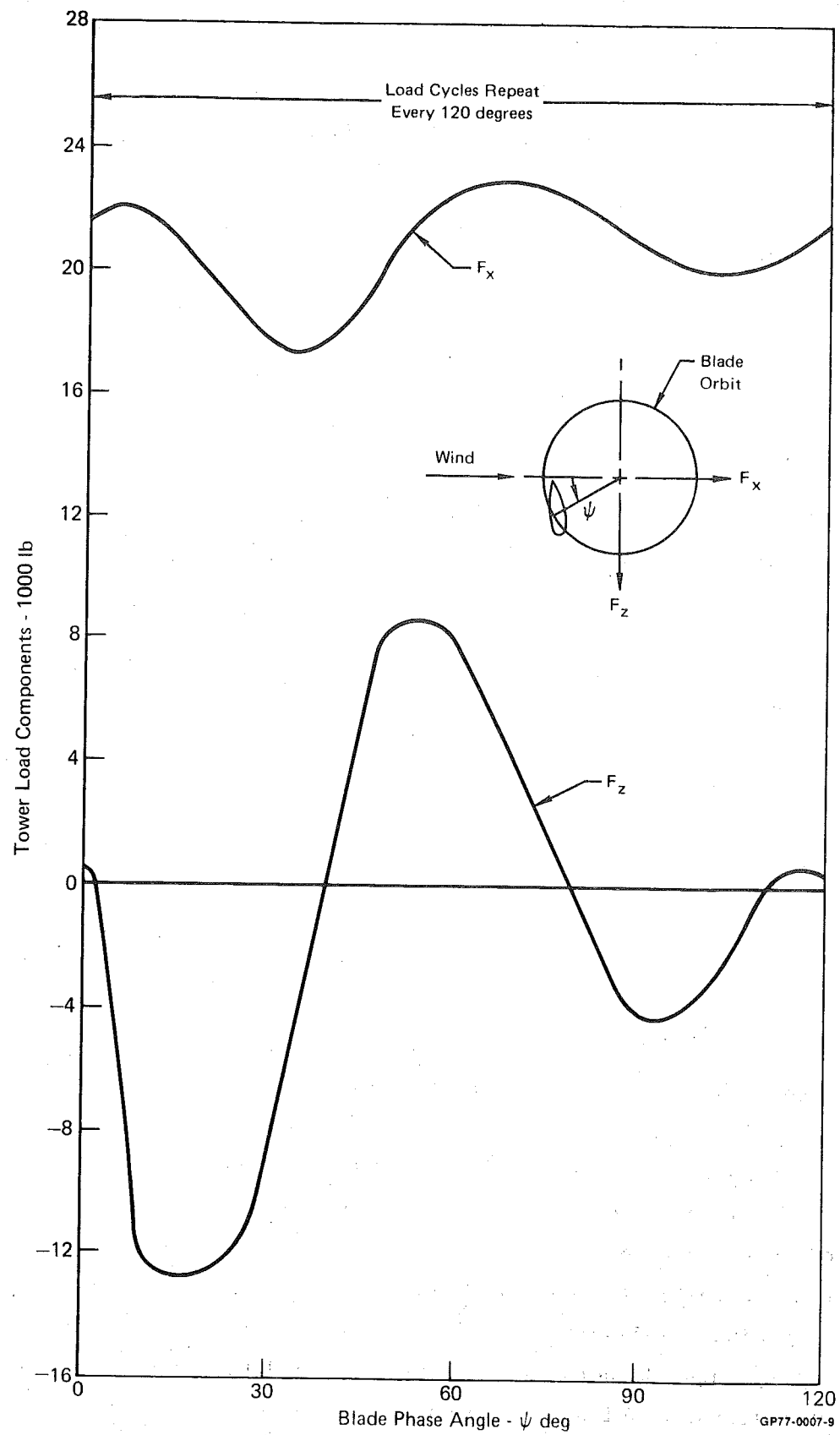


FIGURE 19
TOWER LIMIT LOADS - OPERATING CONDITION

Substructure weights are presented in Figure 20 for Configurations 11 and 11-1. A comparison of blade plus blade support weights indicates considerable weight savings for Configuration 11-1, primarily due to a reduction in the number of blade supports from four to three per blade. The change in high wind condition reduced the sizes required for tower members resulting in a net tower weight savings for Configuration 11-1.

Component	Weight (lb)	
	Configuration 11	Configuration 11-1
Blades	7,350	14,500
Blade Supports	79,100 (4 Blade Supports)	57,100 (3 Blade Supports)
Upper Tower	43,180 (3.75 m Dia)	31,200 (2.62 m Dia)
Lower Tower	26,750	28,800
Total	156,500	131,600

GP77-0007-34

FIGURE 20
CONFIGURATION 11 AND 11-1 STRUCTURAL WEIGHTS

Tower weight is strongly dependent on the wind speed used for high wind load condition, but for realistic sizes the weight is essentially independent of tower cross section size. For example, heavy cornerposts and relatively light diagonals and braces characterize compact tower cross sections. The converse is true for large cross sections. A more compact upper tower cross section is possible for Configuration 11-1 and this enables the use of smaller, and less expensive, tower support bearings. The size of the upper tower cross section, which strongly influences the structural dynamic characteristics of the Giromill, can be "tuned" to provide acceptable dynamic responses without significantly affecting tower weight.

5.5 Structural Dynamics

5.5.1 Structural Dynamics Analysis Overview - The purpose of the structural dynamics investigation was to determine the resonant frequencies and associated mode shapes of vibration of the Giromill system, and to investigate any aeroelastic instabilities that may exist. Vibrations may be divided into two types, ordinary and self-excited. Ordinary vibrations are those in which a system of springs, dampers, and masses is forced to vibrate by some alternating external force which is independent of the motion. The amplitude of the

vibration per unit of applied force may vary widely, depending on the characteristics of the system such as damping and the ratio of the applied frequency to the systems resonant frequency. Vibrations of this type, because of the associated load amplification, are important in determining the fatigue life of the system. In order to avoid a reduction in fatigue life, it is important that no resonances occur at or near the operating point (normal rotational speed) of the system.

Self-excited vibrations are those in which the alternating forces are sustained or controlled by the vibratory motion itself. When self-excited vibrations occur, the system is in an unstable condition and any small disturbance can cause a diverging oscillation. Types of self-excited vibration that can occur in the Giromill system are blade flutter, tower whirl, and coupling of tower bending and support arm horizontal bending. The latter vibration is similar to the ground resonance phenomenon in helicopters. Because of the unstable nature and potential destructive characteristics of self-excited vibrations, it is important to design the system such that these effects do not occur within the operating speed range.

With the Giromill, as with any rotating system, the sources of excitation for vibrations comes from the rotation of the system itself. These excitations can be divided into two types; those due to mass unbalance and those due to aerodynamic imbalance between the blades. The frequencies of these excitations will always be at multiples of the shaft speed and thus are expressed as 1 per rev., 2 per rev., etc. For the Giromill system, these excitations can be characterized as follows:

- 1/rev. excitation - caused by mass and aerodynamic unbalance, this will be a strong input
- 2/rev. excitation - caused by two blade reversals per revolution, also this is the first harmonic of the 1/rev
- 3/rev. excitation - caused by aerodynamic unbalance from the three support arm-blade configuration, this will be a strong input
- 4/rev. excitation - this is a multiple of the two/rev. excitation
- 6/rev. excitation - caused by two blade reversals per revolution in conjunction with three blades, also first harmonic of the 3/rev.

While higher harmonic excitations may be present in the system, it is assumed that their amplitudes will be small enough such that they need not be considered in this study.

In order to simplify the computation of the resonant frequencies of the Giromill system, it was divided into three components or sub-systems; blades, support arms, and tower. The resonant frequencies of these components were calculated and, where appropriate, were then inertially or elastically coupled to give the resonant frequencies of the Giromill system. A short description of each of these resonances and its coupling follows.

Blades - Blade uncoupled vibration modes are flap bending, lag-lead bending, and torsion. Blade torsion must be considered under two conditions, clutched and declutched. With the blade in the clutched condition the pitch change mechanism provides a relatively soft torsional restraint at one end of the blade, and the mode of vibration is essentially rigid blade flexing the pitch change mechanism. In the declutched condition the first torsion mode is blade free-free motion.

Support Arms - Support arm vibration modes can be divided into two types, arm vertical bending and arm horizontal bending. Arm vertical bending can further be divided into symmetrical (all arms responding in-phase) and anti-symmetrical (one arm moving up and the other two moving down and vice-versa). Arm horizontal bending modes can be subdivided into in-phase modes (top, center, and bottom arms moving in the same direction) and out-of-phase modes (top and bottom arms moving in opposite directions with the center arm standing still). These modes can further be described as collective (all three sets of three arms moving in-phase with a resulting torque) or cyclic (a phase of 120 degrees between each set of arms with zero resulting torque).

Tower - Tower vibration modes that were investigated are tower first bending and tower first torsion. Tower first bending must include the effects of foundation flexibilities as well as the tower flexibilities. Tower torsion will be influenced by the polar moment of inertia of the generator gear box combination as well as by the polar moment of inertia of the support arms and blades.

These component modes must be coupled to give total system modes. For example, blade lag-lead bending may couple with support arm horizontal bending. Support arm vertical bending out-of-phase can couple with tower bending. Indeed, many other combinations are possible and were considered in the analysis. This type of an analysis was carried out because at this time the scope of the investigation is simply to determine the feasibility of the Giromill concept. Feasibility of the concept has been proven from a dynamics standpoint

by initially investigating two typical Giromill sizes, a 120 kW and a 500 kW machine (configurations 2 and 12), and then performing it again for the optimized 500 kW configuration 11-1. Only the results of the optimized configuration are presented herein.

5.5.2 Configuration 11-1 Structural Dynamics - The structural dynamics of Configuration 11-1 were determined, and then iterated with the structural design to obtain a natural frequency separation from the operation point. The dynamic characteristics of this configuration are shown in Figure 21. All resonant frequencies except for the upper tower bending and torsion are quite high and are not critical.

Mode	Natural Frequency H_z
Upper Tower Torsion	0.22
Upper Tower Bending	0.34
Blade Torsion	Torsional Support Unknown
Support Arm Tangential Bending (In Phase, Lag-Lead Arm Bending)	1.88
Blade Flap Bending	3.93
Support Arm Vertical Bending (Out of Phase)	5.12
Support Arm Tangential Bending (Out of Phase)	3.39
Support Arm Tangential Bending (In Phase, Blade Mode)	4.23
Support Arm Vertical Bending (In Phase)	2.96

GP77-0007-33

FIGURE 21
SUMMARY OF STRUCTURAL DYNAMICS FREQUENCIES

Figure 22 presents the resonant upper tower bending and torsion frequencies as a function of rotational speed. The points that have strong forced vibrations are indicated by the circled symbols. The operating rotational speed does not pass through any of the forced vibration points, but is close to several. Note also that starting and stopping the Giromill will require passing through several others. The structural ramifications of these resonant frequencies was not con-

sidered in this feasibility analysis. The structural dynamics criteria stipulated was that the natural frequencies and forcing excitations be reasonably separated and that no aeroelastic instabilities exist. This was achieved.

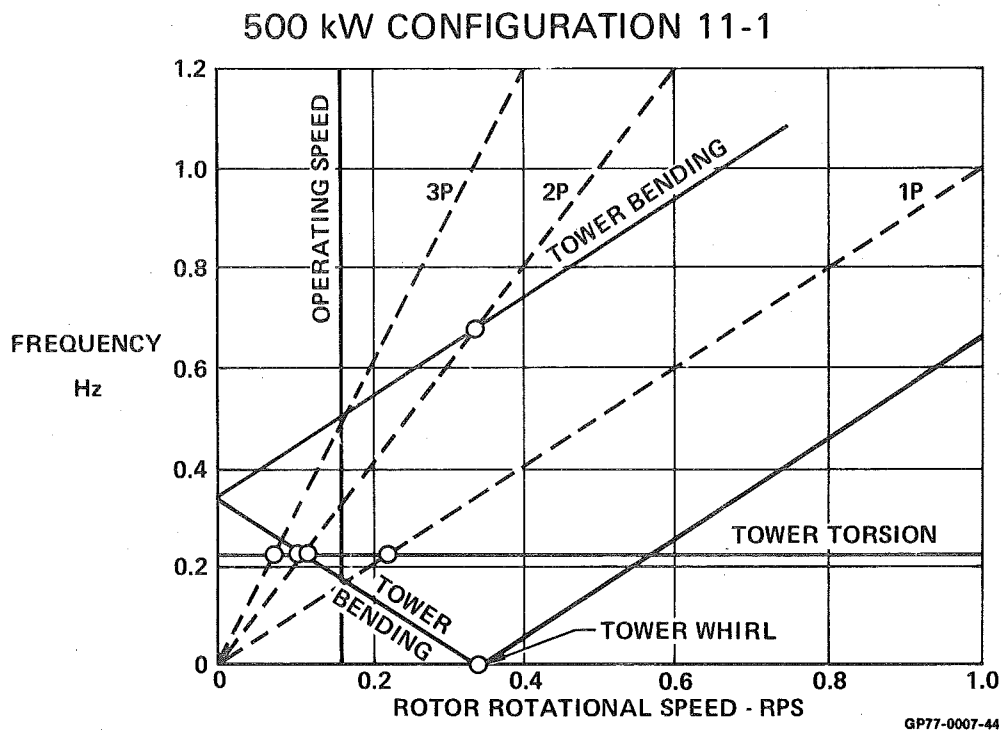


**FIGURE 22
TOWER DYNAMICS**

6. CONTROL SYSTEM

The main functional requirement of the control system is to enable the Giromill to generate the maximum rated power output without exceeding the structural and electrical load limitations. The control system performs this function by controlling the blade rock angles so that the desired Giromill power output is maintained in the presence of wind variations. Other control system functions provide for the start up and power interrupt or shut down situations as they occur to insure that safe operating conditions are met. An electronic control system was selected for this feasibility study since it appeared easier to implement at this time than a mechanical system.

6.1 Control System Functional Operation

The control system must provide the logic to enable the blade actuator to follow the blade rock angle profile determined by the Larsen cyclogiro vortex theory computer program. The blade rock angle profile nominally followed is one that maintains a constant angle of attack, positive over half the blade orbit and negative over the other half. A constant angle of attack, accounting for the variations of the flow field, was determined to be the most efficient. However, the rock angle profile to accomplish this is very erratic, especially for the rearward blade cycle due to the blades traversing the turbulent flow of the forward blades. A function of the control system is to produce a blade rock angle profile that approximates the optimum constant angle of attack by providing a smooth blade modulation.

The requirements of the control system to perform this and the other functions can be described in terms of the condition of the Giromill and the existing wind environment. Figure 23 presents the control system functional diagram. This diagram shows where the various sensor outputs are utilized, provides a tabulation of the switching logic, and indicates the functions that are performed to generate the blade rock angles.

The switching logic that provides for the various operating conditions is detailed in the condition block of Figure 23. Conditions A and B refer to Giromill start up. Conditions C and D indicate that the wind velocity is either too low or too high and the blades should be declutched. Conditions E, F, and G refer to a failure in the Giromill and the system should be shut down until examined and repaired. All other conditions indicate the Giromill is working properly.

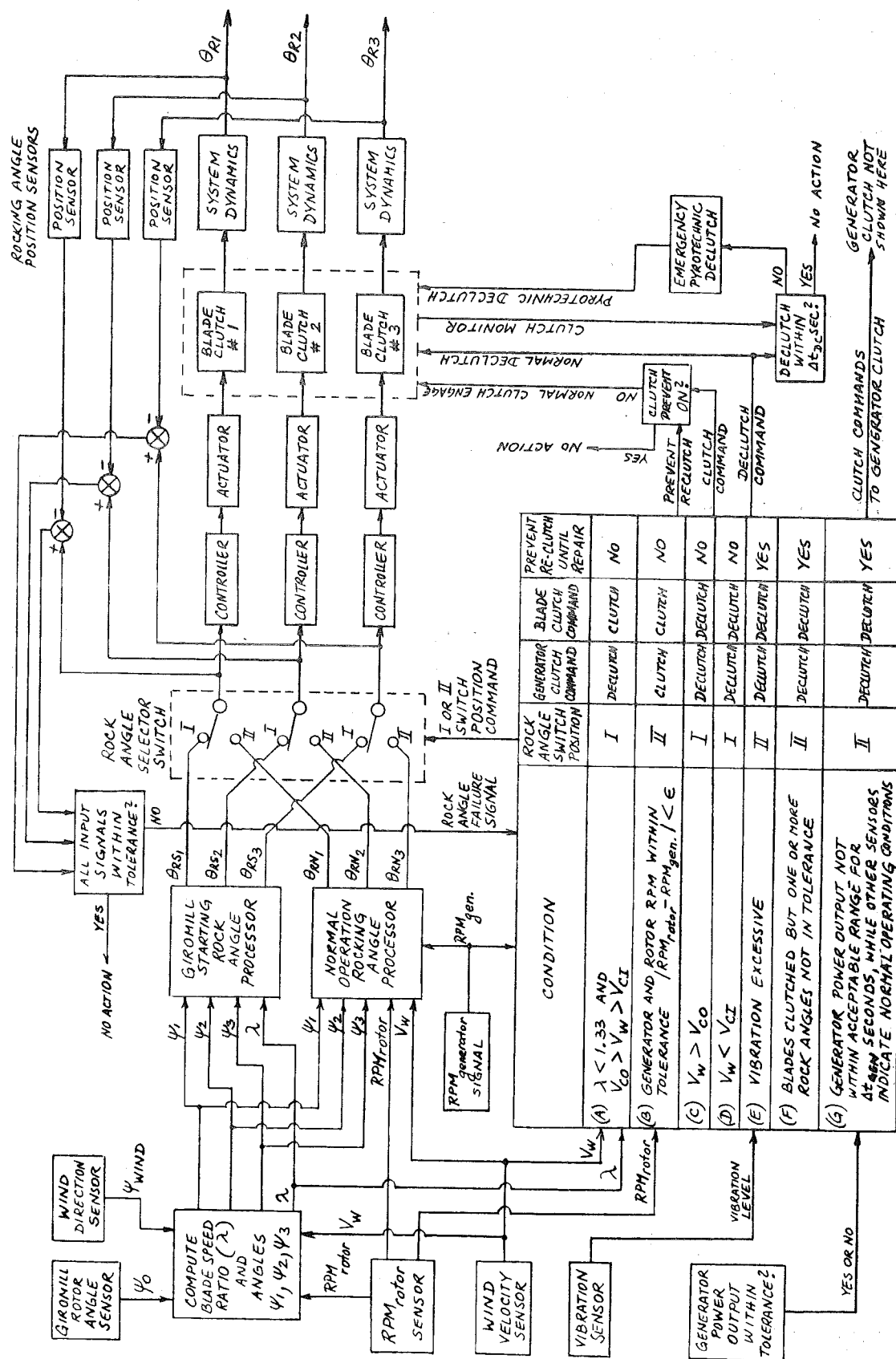


FIGURE 23
GIROMILL CONTROL SYSTEM FUNCTIONAL DIAGRAM

Condition A provides the start up logic; it indicates the wind velocity is adequate and that as long as the blade speed ratio, λ , is less than 1.33, the start up rock angles are being commanded. When λ reaches a value greater than 1.33, the normal operating rock angle processor takes over to continue accelerating the Giromill to the operating RPM. When the Giromill RPM (measured after the RPM speed increaser) is within a specified value, ϵ , from the generator RPM, the generator is clutched in as denoted by condition B.

Conditions C and D indicate the shut down of the Giromill because V_W is greater than the cut off wind velocity V_{CO} , (condition C), or lower than the cut in wind velocity V_{CI} (condition D).

Condition E shuts down the Giromill because the vibration sensor picked up an excessive vibration. This vibration could be due to a rotor unbalance due to blade icing or a structural failure. In any event, the Giromill will shut down and must be manually reset.

Condition F guards against a blade actuator failure. It is possible for one blade actuator to fail and the power loss be made up by increasing the effective angle of attack of the remaining blades. To preclude this possibility, condition F refers to a check between the blade angle commanded and measured. If they are not within a specific value, the Giromill will be shut down.

Condition G is a catch all type of failure detection. If all other conditions are within tolerance, but the generator power is not within an acceptable range for the wind conditions existing at the time, condition G will command a shut down. This catch all condition would detect a generator failure, blade icing that reduced the Giromill efficiency, wind sensor failures, etc.

The Giromill is shut down by merely declutching the blades from their actuator and allowing the blades to weathervane into the wind. It is very important that the blades all declutch. If one blade hangs up the unbalanced forces could cause Giromill destruction. To preclude this from occurring an emergency blade declutching is provided in the form of a pyrotechnic shearing of the shaft connecting the blade to the actuator. This is also shown in the functional diagram of Figure 23.

6.2 Blade Rock Angle Control Implementation

The previous section provided a brief description of the functional operation of the control system. This section amplifies the description by defining the technique for implementing the blade rock angle that drives the Giromill.

The blade rock angle computed by the cyclogiro vortex theory computer

program is for maintaining a specified α_e . This usually results in some large rock angle excursions as the blade passes near a shed vortex. One of the functions of the control system is to smooth this rock angle while performing the other functions previously described.

The rock angle implementation within the control system was incorporated as shown functionally in Figure 24, and in more detail in Figure 25. The implementation consists of computing the blade rock angle for zero angle of attack and no induced effects (θ_{R0}), and successively modifying this rock angle to account for the desired α_e and the induced α_i . Equation wise this can be expressed as:

$$\theta_R = \theta_{R0} + (C_{\alpha_i})(\alpha_i)_{Ref} - (C_e)(|\alpha_e|)$$

where:

C_{α_i} is an induced angle of attack correction coefficient given as a function of $\alpha_e/\alpha_{e_{max}}$

$(\alpha_i)_{Ref}$ is the induced angle of attack at $\alpha_{e_{max}}$

C_e is the α_e profile coefficient given as a function of blade phase angle ψ .

A generator power condition is fed back to make an incremental blade rock angle correction to keep the power output within specification.

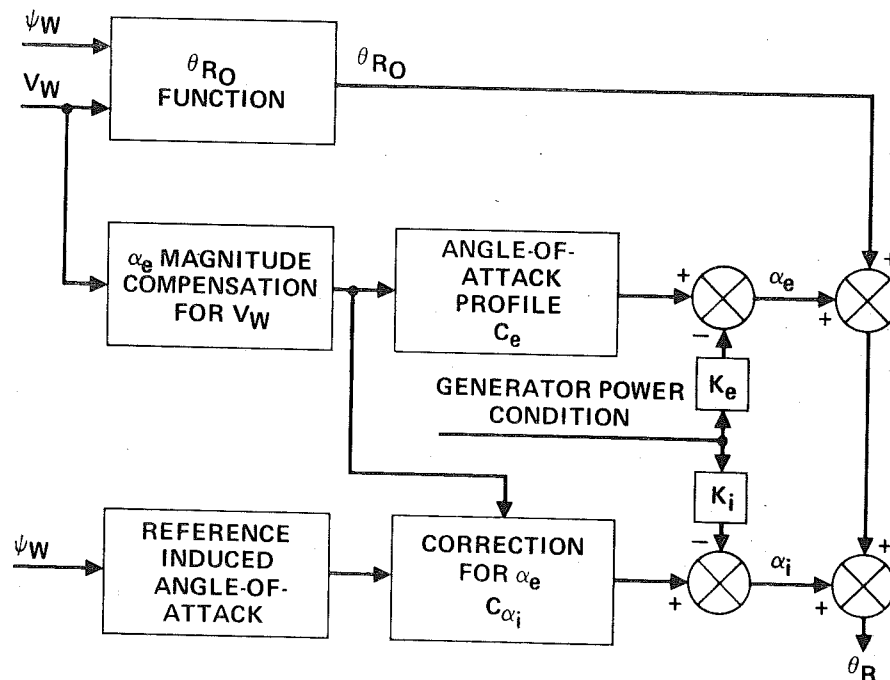
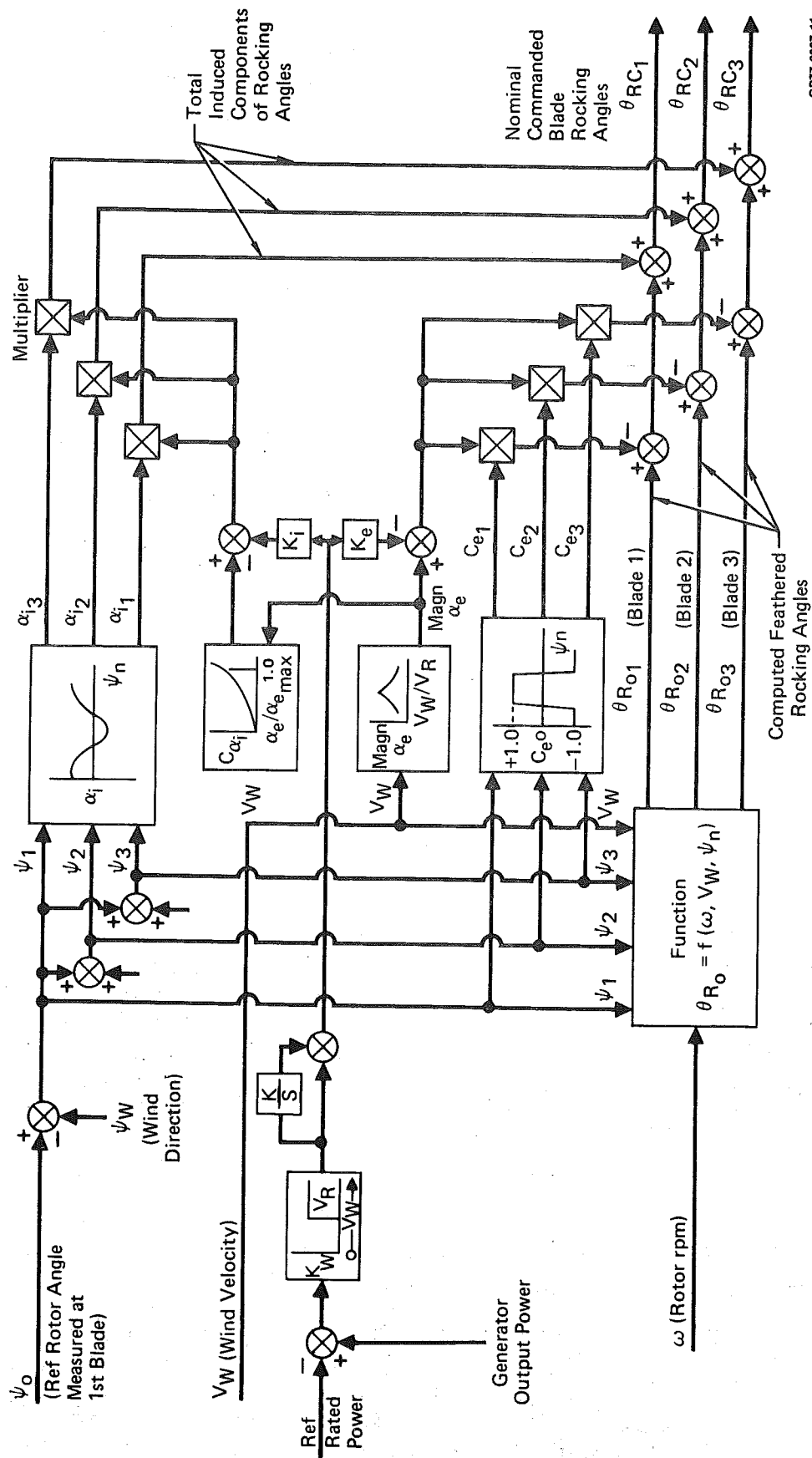


FIGURE 24
BLADE ROCK ANGLE CONTROL
FUNCTIONAL REPRESENTATION

GP77-0007-45



GP77-0007-11

FIGURE 25
BLADE ROCK ANGLE CONTROL IMPLEMENTATION

The equation that relates the blade rock angle for zero angle of attack assuming no induced effects is:

$$\theta_{R0} = \arctan \left[\frac{-\cos\psi}{\frac{\omega R}{V_W} - \sin\psi} \right]$$

where:

ψ - Blade phase angle

ωR - Blade rotational speed

V_W - Wind velocity

This computation is denoted in the block denoted by $\theta_{R0} = f(\omega, V_W, \psi_n)$ in Figures 24 and 25. The numbers 1, 2, or 3 after the various symbols refer to the three blades.

The θ_{R0} thus computed for the three blades are then modified for the desired effective angle of attack α_e . The nominal magnitude of α_e is obtained from Figure 10. This figure shows how α_e nominally varies with V_W to maintain constant power and RPM when $V_W > V_R$, and max power at constant RPM when $V_W < V_R$. This α_e magnitude is then related to the desired α_e profile by multiplying by the coefficient C_e . This then provides a rock angle that would give the desired α_e around the rotor but neglects the induced effects.

The induced effects are determined by using as a reference the induced effects α_i computed by the vortex theory program at the maximum effective angle of attack $\alpha_{e_{max}}$ conditions, and then correcting it for the actual value of α_e being commanded at that time. This correction was determined empirically using the vortex theory program, and takes the form of a multiplying constant, C_{α_i} , determined as a function of the actual $\alpha_e / \alpha_{e_{max}}$ existing at that time. This was checked out over the range of wind velocities expected, and predicted quite accurately the expected α_i . Since a smooth reference α_i is used, this also smooths the final blade rock angle, θ_R , computed. The results of applying this technique are illustrated in Figures 26, 27, and 28.

Figure 26 shows the reference induced angle of attack as computed by the vortex theory and smooth hand faired curve. Figure 27 presents the C_{α_i} correction empirically determined as a function of $\alpha_e / \alpha_{e_{max}}$. This curve assumes that $\alpha_{e_{max}}$ is commanded at the rated wind conditions. Figure 28 shows a typical example of how well this technique works. This is for a case where α_e would be 4.7° to maintain constant power and RPM, and for this Giromill $\alpha_{e_{max}} = 9^\circ$ at $V_W = V_R$ so that $\alpha_e / \alpha_{e_{max}} = 0.52$. The power output using the control system computed rock angle was about 9% high, and would have been reduced using the

generator output power condition feedback loop to incrementally correct α_e and α_i to get back to the desired power. It does this through use of an empirically determined gain K_w , which is a function of wind velocity, acting on the power output error through a proportional integral feedback circuit.

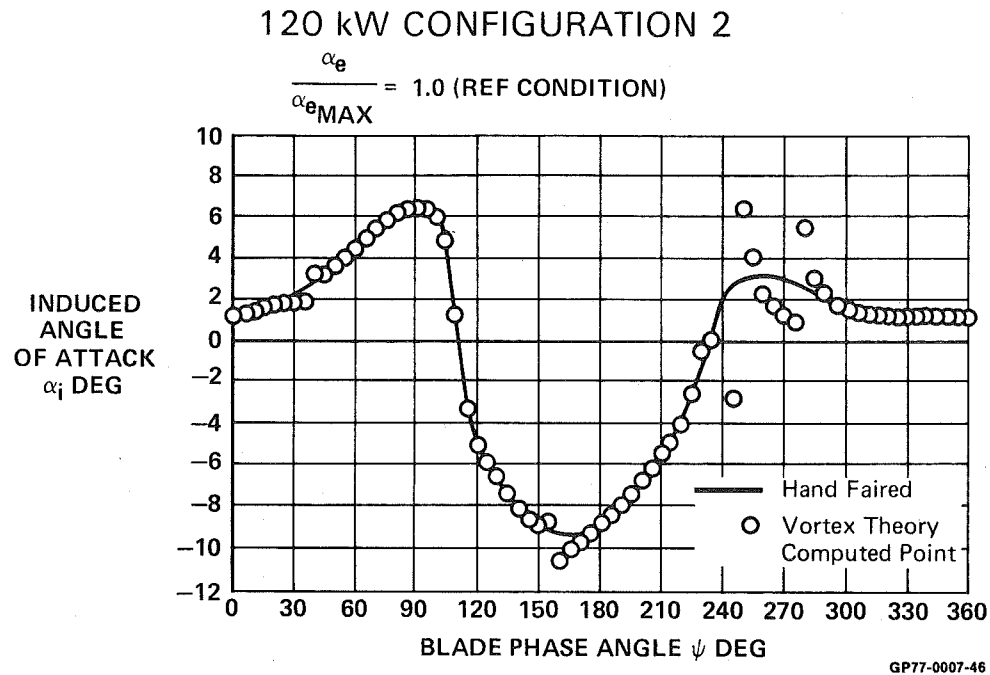


FIGURE 26
INDUCED ANGLE OF ATTACK ALONG THE BLADE ORBIT

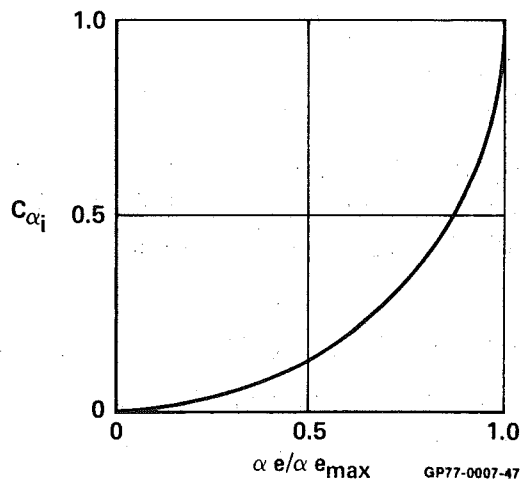
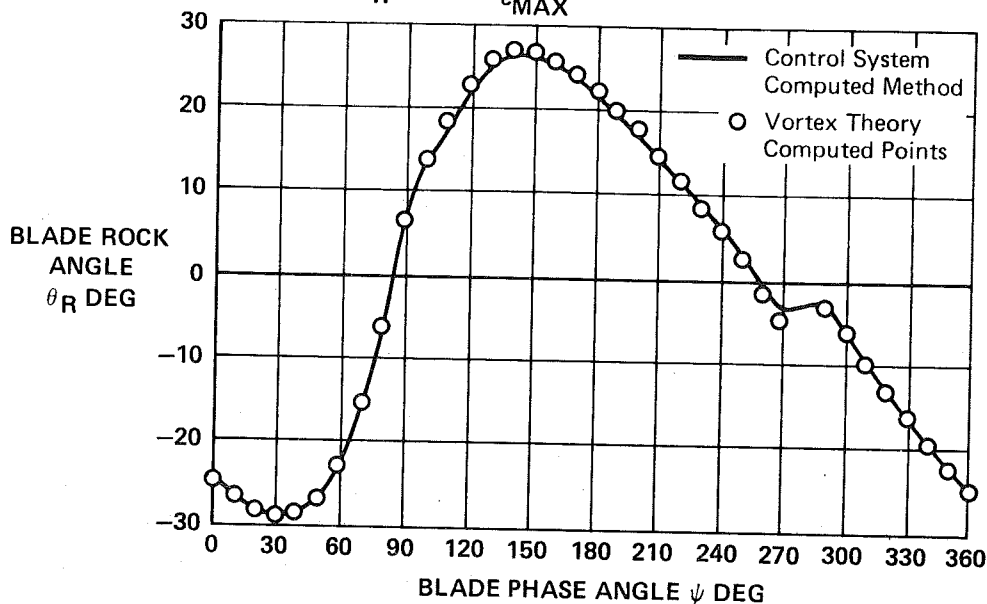


FIGURE 27
**INDUCED ANGLE OF ATTACK COEFFICIENT
VARIATION WITH WIND VELOCITY RATIO**

120 kW CONFIGURATION 2

$$\frac{V_R}{V_W} = 0.7, \frac{\alpha_e}{\alpha_{eMAX}} = 0.52$$



GP77-0007-48

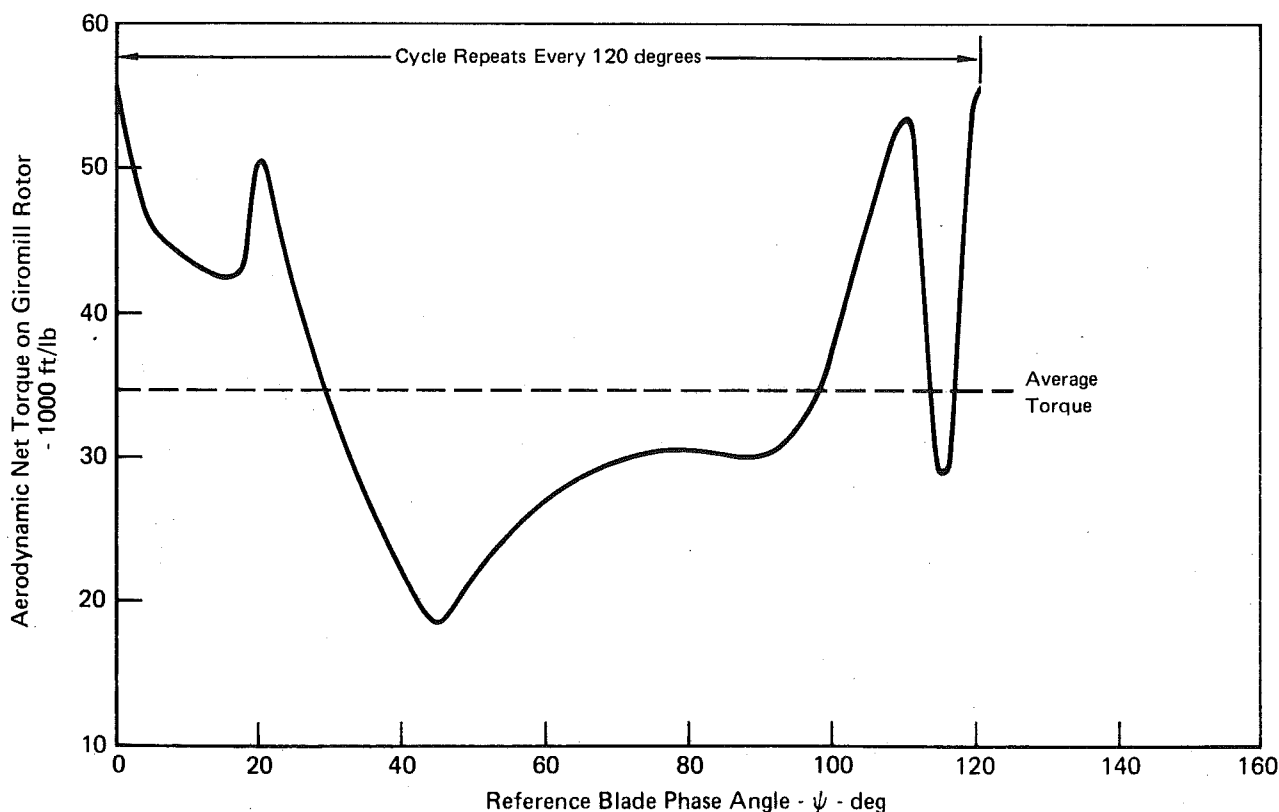
FIGURE 28
ROCK ANGLE COMPUTATION COMPARISON

6.3 Effect of Aerodynamic Net Torque Variation on Rotor RPM

The Giromill blade rocking angles are positioned so that the magnitudes of the effective blade angles of attack at a given wind velocity are essentially constant at all times. However, in order to produce the desired aerodynamic torque on the rotor the sign of the angle is reversed twice during each revolution so that the angle of attack is alternately positive and negative in the aft and forward half-cycles, respectively. This scheme is very efficient in generating high average torque on the rotor, however, the net aerodynamic torque varies considerably while the rotor is turning. This section reports on the torque variation and its effect on the rotor RPM assuming no control system feedback or synchronous generator is used. This analysis was done to acquire an insight of the generator synchronization problems which may arise due to this torque variation.

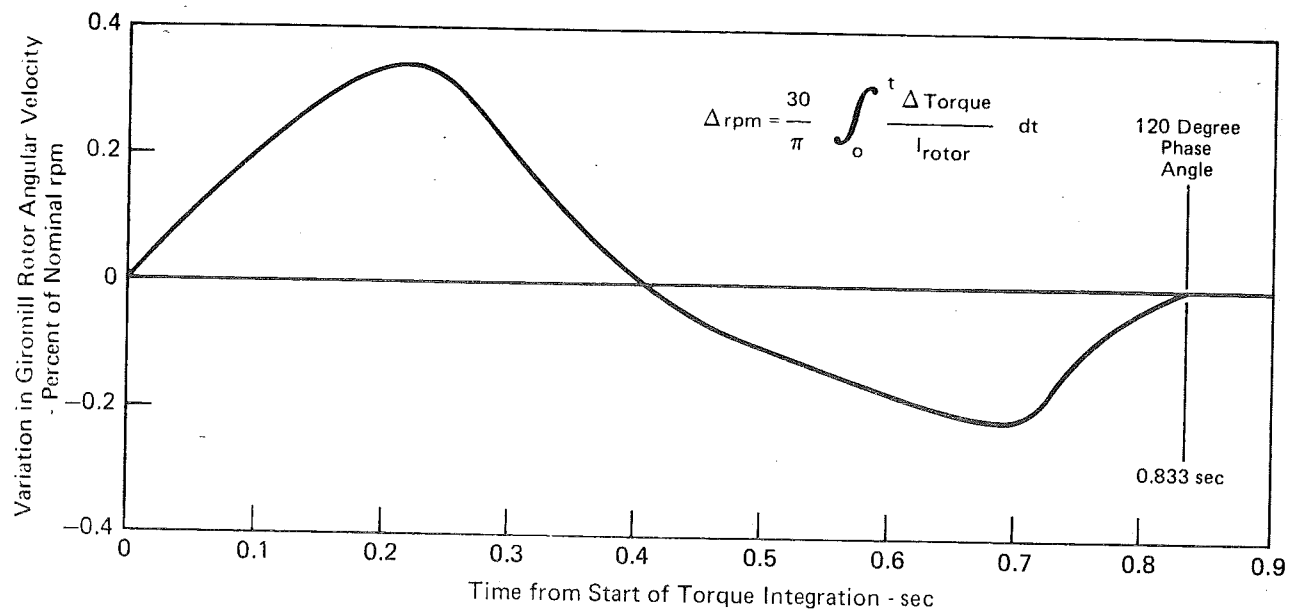
The torque and RPM data used here are based on the 120 kW Configuration 2. This configuration is a three-bladed Giromill having 24 RPM nominal angular velocity. The Giromill rotor axial moment of inertia for this configuration is 243,400 slug ft².

With no dynamic effects and with no control corrections included, the net aerodynamic torque for a steady state operating condition is represented by Figure 29. The steady state aerodynamic net torque exactly balances the average friction and load on the rotor. The rotor angular acceleration was determined from the variations in aerodynamic torque and integrated to obtain the resulting variations in rotor RPM as function of the rotor phase angle. This change in rotor RPM, computed as a percent change from the nominal rotor RPM, is presented in Figure 30 and shows that the Giromill RPM variations due to aerodynamic torque variations are relatively small, being less than 0.6 percent (+0.35% and -0.25%) of the nominal rotor RPM.



GP77-0007-12

FIGURE 29
CYCLIC TORQUE VARIATION



GP77-0007-13

FIGURE 30
ROTOR ANGULAR VELOCITY VARIATION

No attempt was made, at this time, to quantify this torque variation and that due to wind gust effects on the operation of the synchronous generator within a power grid. The problems of integrating a Giromill in a power grid are not expected to be much different than a conventional windmill.

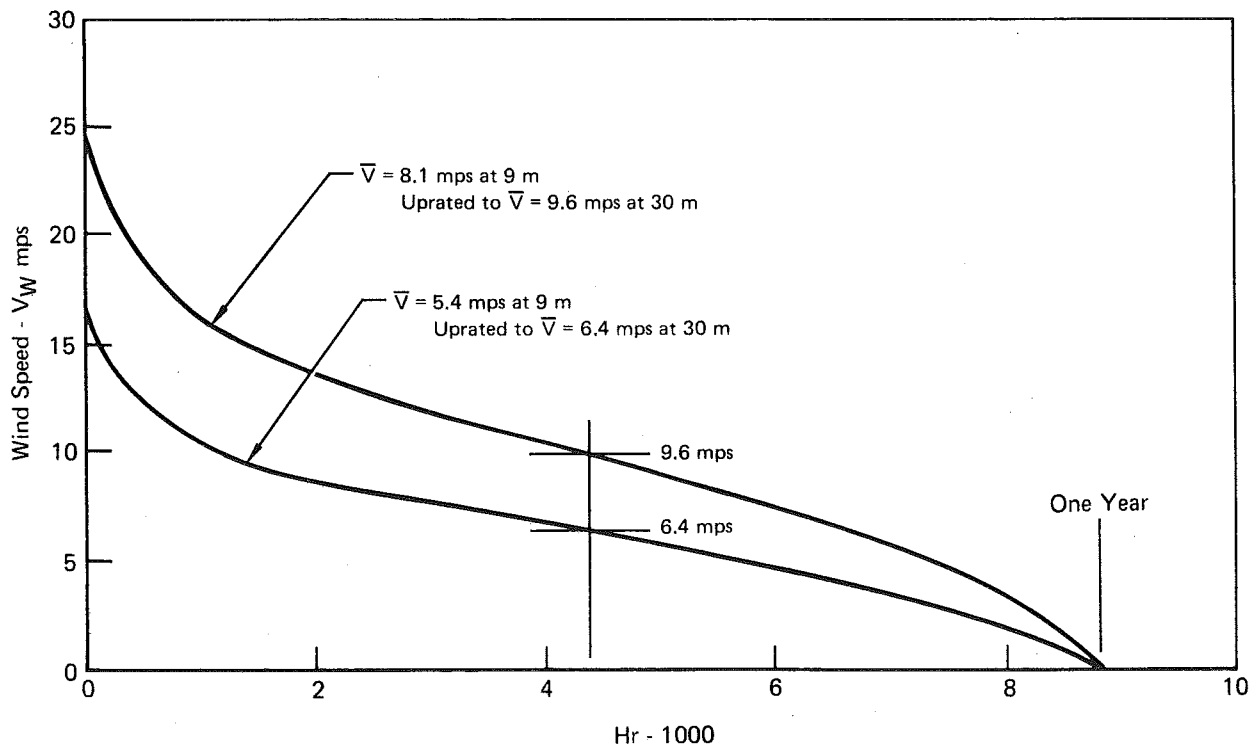
7. ENERGY OUTPUT EVALUATION

7.1 Wind Duration Curves

The study ground rules specified two typical wind speed distributions for the Giromill parametric analysis. One distribution having a mean wind speed of $\bar{V} = 5.4$ mps (12 mph) was used for the 120 and 500 kW systems, and a second with $\bar{V} = 8.1$ mps (18 mph) was used for the 1500 kW systems. These winds are specified at an altitude of 9 m (30 ft), and have to be uprated to an average height of the Giromill. For simplicity this average height was always taken as 30 m (100 ft). The 1/7 power law for wind velocity with altitude was used:

$$V_{30\text{ m}} = V_{9\text{ m}} \times \frac{30\text{m}}{9\text{m}}^{1/7} = 1.188 V_{9\text{ m}}.$$

These uprated wind velocity curves used for determining the Giromill power output are shown in Figure 31.



GP77-0007-14

FIGURE 31
UPRATED WIND SPEED DURATION CURVES

7.2 Energy Output

Giromill energy output is obtained by integrating the Giromill power output characteristics over the wind duration curves. The Giromill power output characteristics for a given size system can be considerably modified by rotor solidity and the wind velocity magnitude where $C_{p_{max}}$ is achieved. The beneficial performance effect of the lower solidity of the optimized 500 kW system, configuration 11-1, was previously discussed in Section 3.2. This increased the yearly power output of 11-1 by 3% over the value initially calculated for configuration 11, and reported in our mid-term report, using a power curve derived from a higher solidity system.

These power calculations assumed that $C_{p_{max}}$ was achieved at the rated wind velocity, V_R , of the system. Power output optimization has shown that a greater yearly power output can be achieved by shifting the operating performance so that $C_{p_{max}}$ occurs at a wind velocity less than V_R . What this means is that the integration of the higher C_p values, over the longer time duration of the lower wind velocities, gives a greater yearly energy output. This operating point change is physically accomplished by a slight reduction of the design rotor RPM such that the blade speed ratio for $C_{p_{max}}$, which has not varied, now occurs at a wind velocity 85% of V_R . Another 3% increase in yearly energy output can be gained by this optimization providing a total increase of 6% over the values quoted in our mid-term report - from 1.49×10^6 to 1.574×10^6 kW hr./year for configuration 11 and 11-1.

The power values obtained for the various Giromill systems analyzed are summarized in Figure 42 on page 56.

8. COST ANALYSIS

This section discusses the total production costs and operating and support (O&S) cost components associated with the Giromill subsystem. These have been developed for production unit 100 and considering a design life of 50 years for static components and a design life of 30 years for dynamic components, e.g., rotor blades.

Costs considered in the life cycle of a new system are generally comprised of the following elements.

- (1) Research, Development, Test and Evaluation (RDT&E)
- (2) Production (includes purchase and preparation of land)
- (3) Recurring Costs (cost of capital and operation and support (O&S))

RDT&E and production costs comprise total program or acquisition costs. The present study will not address RDT&E elements but will concentrate on identifying the production and O&S costs.

Production costs include the cost of the various components and raw materials comprising the Giromill system, fabrication of raw materials, assembly and installation of the entire system. In addition, these costs include cost of special support equipment (SSE), if necessary, and cost of acquisition of the land, site preparation, and provision for security. The present analysis is intended as a feasibility assessment, and does not assume a specific application for the Giromill system such as a power generating source to be input to an existing electrical power plant. Consequently, the cost to hook-up to a power generating source using transformers, cables, and other equipment is not considered in this analysis.

Two major areas of recurring costs to be considered are cost of capital and other operation and support (O&S) costs. The cost of capital includes the categories typically called investment charges, i.e., interest on bonds, dividends, depreciation, income taxes, and insurance. This cost of capital represents a large share of the cost of generating electricity and it is common practice to estimate these costs as a percentage of the total cost of the system installation.

Operation and support costs consider those components of direct personnel or labor, spare parts, supplies, and supervision. For a conventional electrical generating facility, fuel costs are a major component of the operating costs. The basic structure of O&S costs will be addressed in this section.

For cost analysis purposes, the Giromill is assumed comprised of several interacting subsystems. These subsystems are:

- ° Foundation and Tower Structure
- ° Electrical Components
- ° Mechanical Power Transmission
- ° Blades and Blade Supports
- ° Blade Control

Individual components of these various subsystems are identified below. In cases where off-the-shelf components are available, the vendor costs have been obtained and used to derive cost estimating relationships (CER), adjusted to 1975 dollars, relating cost with size, weight, power requirements or other physical and/or performance characteristics. These identified relationships are subsequently used in production costs. Engineering judgement is utilized to assess production costs of non-shelf items such as the foundation and tower structure and the blade supports. McDonnell Aircraft Company producibility personnel were consulted to determine the material cost for the tower and both material and fabrication costs associated with developing the blade system. Considerable emphasis was placed on the design of the blade control system and cost estimates for producing this system were determined by McDonnell Douglas Electronics Company.

Subsystem and component costs are discussed in Section 8.2. The total cost of producing energy for the 120 kW and 500 kW systems are presented in Section 8.3. Total production costs (dollars), system cost per rated output (dollars/kW) and cost per annual energy output (cents/kWhr) are presented in that section. Point design configurations were investigated, and their system costs determined.

8.1 Basic Cost Elements

Basic cost elements discussed in this section are those components of cost that are related to the total system and are not identifiable with a specific component or subsystem. These cost elements are (1) cost of capital, (2) incidental costs, and (3) operation and support costs.

Cost of Capital - The cost of capital for the Giromill installation will be based on a percentage of the total system installed cost. A rate of 15% of the total installed cost per year is assumed to cover the following annual charges:

- ° Depreciation
- ° Cost of indebtedness, interest on bonds and notes
- ° Federal income taxes
- ° State and local taxes
- ° Cost of equity, common and preferred stock

Figure 32 illustrates a possible financing structure for a Giromill system resulting in the aforementioned 15% annual cost of capital. The total financing as shown is comprised of bonds (60%), preferred stock (10%) and common stock (30%). The 15% Cost of Capital agrees with values used for other current wind power generation programs.

Element of Cost of Capital Analysis (Annual)	Portion of Installed System Cost
Income Generated	0.15000
Less: Depreciation (30 Years)	0.03333
Less: Bond Interest	0.04800
Income Before Taxes	0.06867
Less: Federal Income Tax at 48%	0.03296
Income After Taxes	0.03571
Less: State and Local Taxes at 4%	0.00143
Less: Preferred Stock Dividends	0.00800
Common Stock Equity	0.02628
Return on Common Equity	8.76%

Assumed Capital Structure:
 60% Bonds at 8% Interest
 10% Preferred Stock at 8% Dividend
 30% Common Stock

GP77-0007-32

FIGURE 32
COST OF CAPITAL ANALYSIS FOR TYPICAL
CAPITAL STRUCTURE

Incidental Costs - The incidental cost of final assembly and total shipping costs are assumed at 10% of the costs for all subsystem components. At the subsystem level some installation and fabrication costs have already been included for such elements as the tower and blade supports and rotor blades. For example, both tower and blade support structure are assumed as \$1.00/lb, whereas the cost of the channels and I-beams comprising most of the tower structure is on the order of \$.13 to \$.16/lb and pipe for the blade supports on the order of \$.22/lb.

Operations and Support Cost - Annual operations and support cost are assumed to be 4% of the total Giromill installed cost. Specifically, the following elements will be considered:

- ° Salary for maintenance and supervisory personnel
- ° Maintenance and overhaul costs
- ° Administrative and general expenses
- ° Insurance
- ° Miscellaneous expendables

This value of 4% is conservative when compared with O&S costs for electrical utilities but consistent with those for other wind power generation programs.

8.2 Production Costs for Giromill Subsystems

Production costs discussed in this section will include the following cost elements:

- ° Raw materials
- ° Off-the-shelf components
- ° Manufacturing and assembly costs
- ° Purchase and preparation of land, security provisions

The production costs are based on costs associated with the Giromill production unit 100 and based on 1975 prices. For cost analysis purposes it was assumed that all manufactured components, such as rotor blades, are manufactured within a time span of three years. Costs for major off-the-shelf components such as generators, speed increasers, couplings and bearings were obtained either from vendor catalogs or from the vendors directly. Cost estimating relationships (CER) were developed for some of these components to permit efficient calculations for point design analyses of the Giromill systems. The following Giromill subsystems are discussed below.

- ° Foundation and tower structure
- ° Electrical components
- ° Mechanical power transmission
- ° Blades and blade supports
- ° Blade control

Foundation and Tower Structure - Cost analysis for the foundation and tower structure began with selection of the appropriate Giromill tower structure, i.e., concept, weight, material. An inexpensive carbon steel, such as A36, was selected for this structure with I-beams and channels for the major

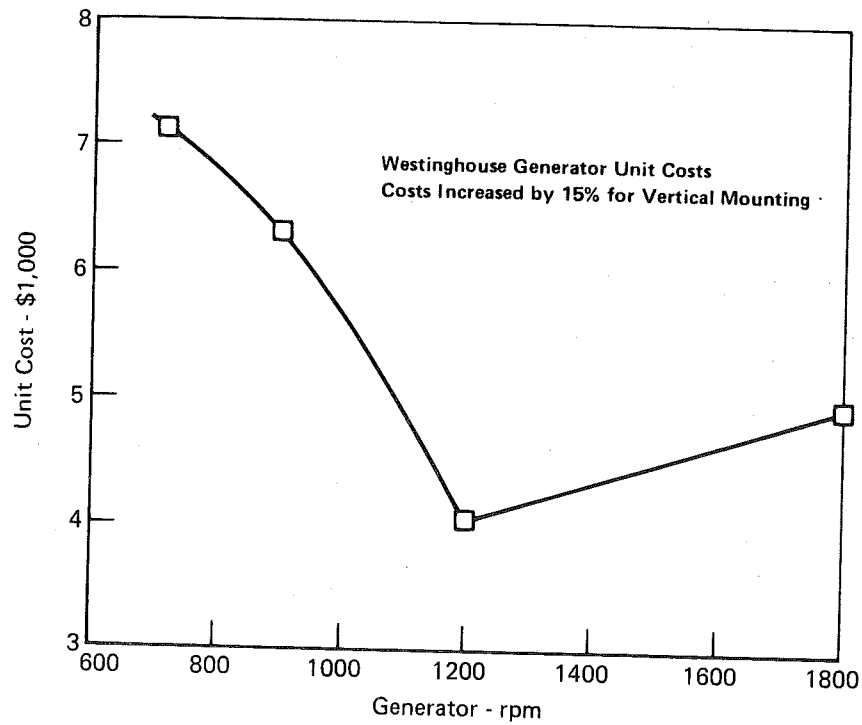
structural members. Final assembly at the site will require welding and/or bolting to join the members. Raw material costs were obtained for typical channels and I-beams, and from these cost per pound of material was determined for large quantity purchases. Final tower assembly was initially based on a total of \$1.00/pound for material and installation. The Giromill costs shown in the charts of the next section use this \$1.00 per pound value. Subsequent to these analyses we had consultation with Union Electric utility tower design personnel. They indicated that they used a value of \$0.50/pound for their large towers. Also, a review of the Kaman data presented in their July 1975 Design Review shows they used \$0.695/pound. On the basis of this the structural steel costs for configuration 11-1, the 500 kW system optimized, was taken as \$0.75/pound.

Cost of tower foundation for the 120 and 500 kW systems has been estimated as a fraction of tower costs. A value of 25% of the tower cost, e.g., both the lower tower and the upper rotating tower, was assumed for the foundation. For the 1500 kW system a revised method that appeared more in line with accepted practice was employed. This based the cost of the foundation as 15% of the total weight of the tower (both upper and lower) blades, and blade supports.

Electrical Component Costs - The electrical components as well as some components of the mechanical transmission will be protected from direct contact with the environment by a simple shroud. Consequently, they will not be totally protected from the environment and may experience temperature extremes, for example, from -40°F to 120°F, depending upon location. No environmental control system (ECS) or heaters for the generator are considered. The major cost components for the electrical system is the generator. In addition, a voltage regulator and simple control panel and indicators will be required.

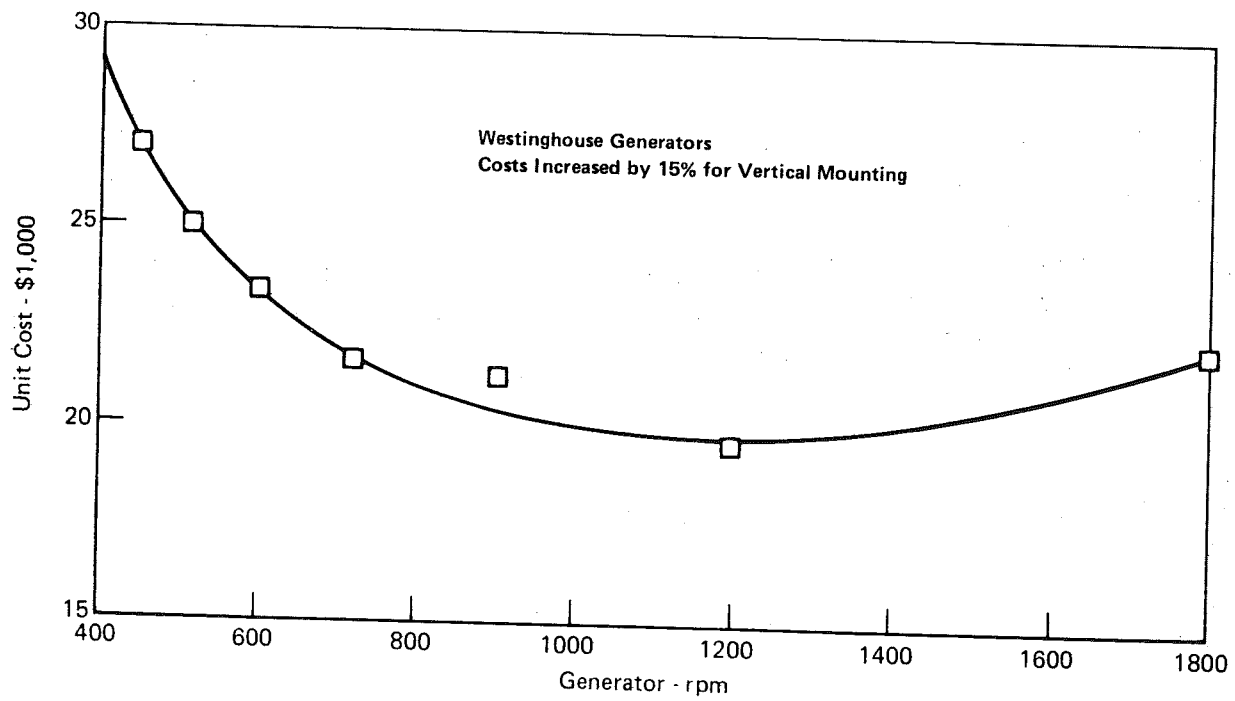
CER's were developed for 100 to 150 kW and 500 kW generators and are shown in Figures 33 and 34. A 15% increase over vendor data costs was applied to these data to account for the higher cost of mounting the generator vertically. Cost data were not available for the 1500 kW system but were projected from the 500 kW system by scaling up by a factor of approximately 2.15.

The total cost of all electrical components other than the generator was assumed to be the same for all systems and was calculated at \$4025.



GP77-0007-15

FIGURE 33
COST RELATIONSHIP FOR 100 TO 150 kW SYNCHRONOUS GENERATOR



GP77-0007-16

FIGURE 34
COST RELATIONSHIP FOR 500 kW SYNCHRONOUS GENERATOR

Mechanical Power Transmission - The mechanical power transmission system

primary components include:

- RPM speed increaser
- Couplings - generator to speed increaser and speed increaser to drive shaft
- Bearing - combination on drive shaft
- Adaptor - shaft to rotor
- Drive shaft

CER's developed for these major components of the mechanical power transmission are shown in Figures 35 through 38. The speed increaser cost shown in Figure 35 and used in the Giromill cost charts in the next section have been increased by 15% over vendor data to account for the additional expenses of vertical mounting. Further information from the Falk Corp. indicated 15% was high, so this value was reduced to 10% for the configuration 11-1 optimum design cost analyses. As shown, the speed increaser cost increases as the gear ratio increases, i.e., as the Giromill rpm decreases. This was considered and traded off with generator cost in costing alternate point designs. The 1500 kW system speed increaser costs shown in the next section were based on a value of \$42,000 quoted by a representative of the Falk Company, and increasing this value by 15% to account for vertical mounting.

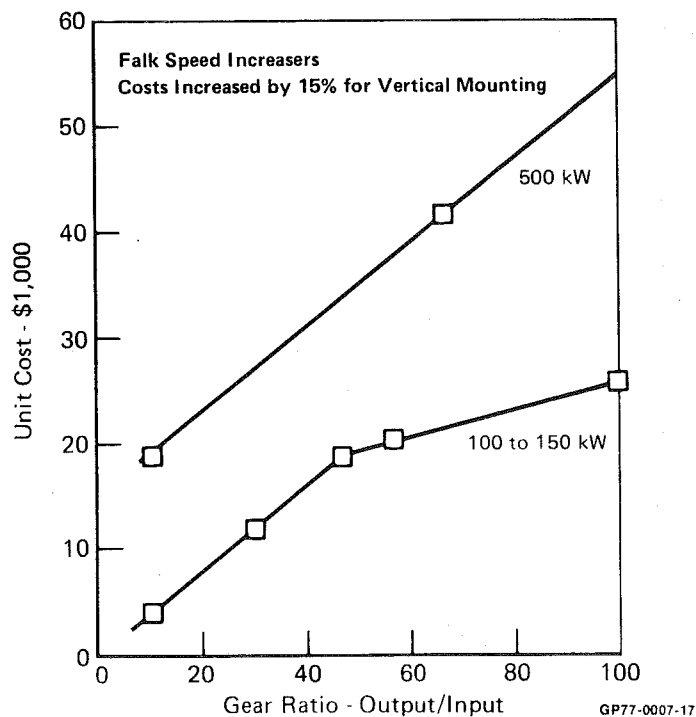


FIGURE 35
COST RELATIONSHIPS FOR 100 TO 150 kW AND 500 kW SPEED INCREASERS

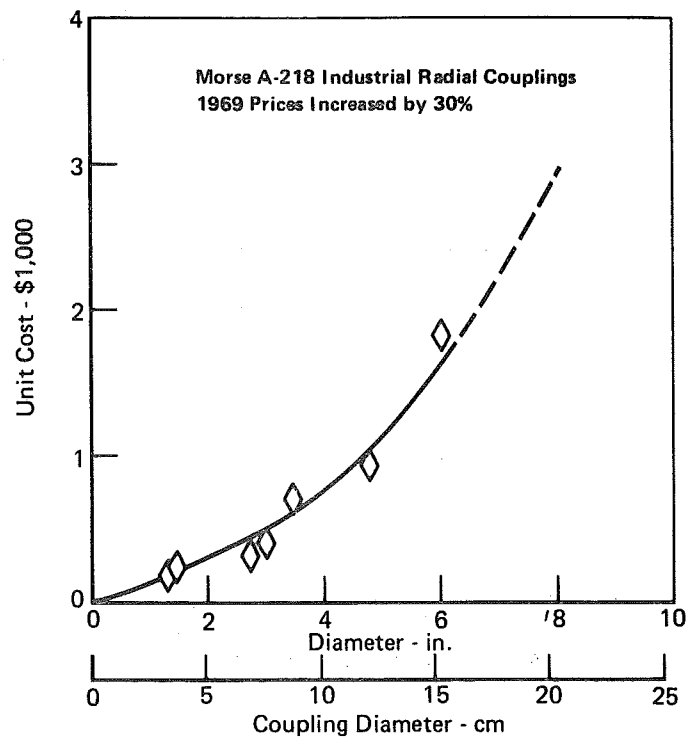


FIGURE 36
COST RELATIONSHIP FOR FLEXIBLE COUPLING

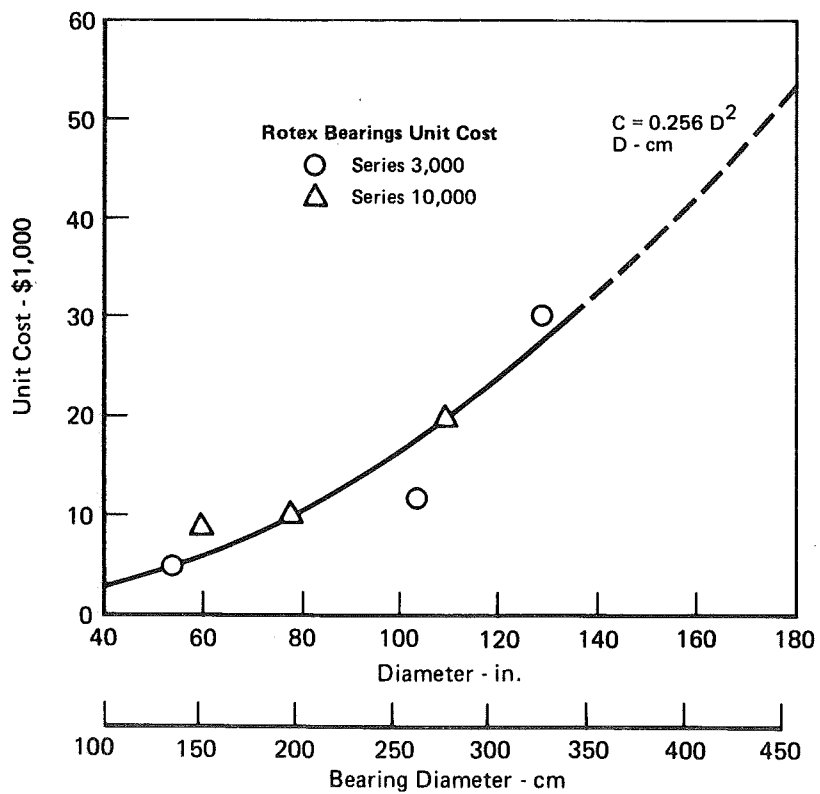


FIGURE 37
COST RELATIONSHIP FOR LARGE DIAMETER COMBINATION BEARING

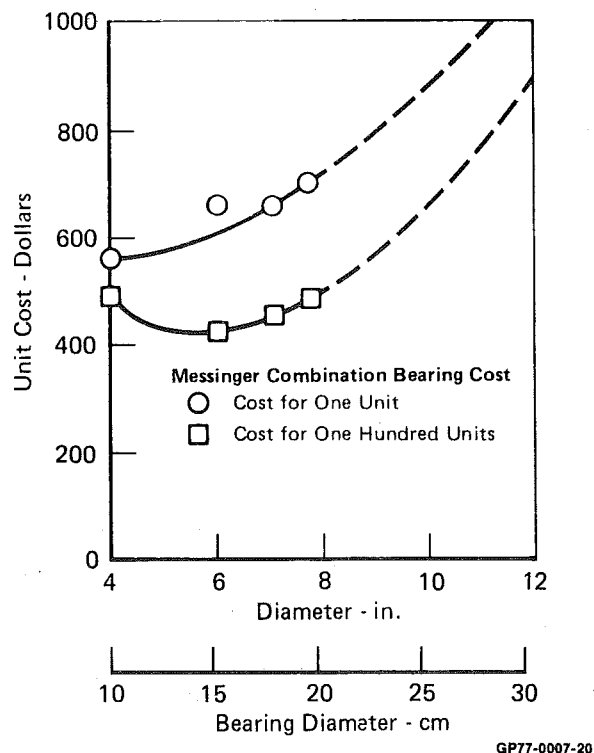


FIGURE 38
COST RELATIONSHIP FOR SMALL DIAMETER COMBINATION BEARINGS

Costs for couplings versus diameter are shown in Figure 36; costs for bearings versus diameter are shown in Figures 37 (large size) and 38 (small size). Cost versus diameter for the couplings is also utilized in determining the shaft to rotor adaptor cost. Figure 39 summarizes characteristics, weight, cost, and cost per unit weight for the components of the 120 kW and 500 kW system. With the exception of the speed increasor, whose cost varies with Giromill rpm, the costs for all components described in Figure 39 are the same for all point designs with the same Giromill output power. A detail analysis of these components for the 1500 kW system was not accomplished. Costs for these components for the 1500 kW system were projected from data on the 500 kW systems by using a factor of 2.5 times the cost of the components for the 500 kW systems and rounding to the nearest \$1000.

Blade and Blade Support - The fabrication of rotor blade supports emphasizes the use of simple member types (tubular cross section) and an inexpensive material, for example, A36 carbon steel. This approach enables the support members costs to be approximated by the tower structure cost of \$1.00/lb initially and \$0.75/lb for the optimized configuration.

- 120 kW Configuration 2
- 500 kW Configuration 14

Component	Characteristics 120 kW First Line 500 kW Second Line	120 kW			500 kW		
		Weight (lb)	Cost (\$)	\$ (lb)	Weight (lb)	Cost (\$)	\$ (lb)
Speed Increaser*	Gear Ratio 50:1 (1,200 rpm) Gear Ratio 22.8:1 (450 rpm)	7,100	19,000	2.68	8,955	24,000	2.68
Coupling - Generator to Speed Increaser	3.5 in. dia 6.42 in. dia	128	640	5.00	366	1,860	5.08
Flexible Coupling - Gen. to Drive Shaft	7.25 in. dia 13.29 in. dia	600	2,400	4.00	2,016	8,064	4.00
Adaptor - Shaft to Generator	7.25 in. dia 13.29 in. dia	188	877	4.67	632	2,947	4.67
Drive Shaft	6 in. O.D., 4 in. I.D. x 12 in. 11 in. O.D., 9 in. I.D. x 12 in.	53	106	2.00	107	214	2.00
Thrust/Radial Bearing	6 in. dia 11 in. dia	42	420	10.00	78	780	10.00
Total (Excluding Speed Increaser)		1,011	4,443	4.39	3,199	13,865	4.33

* Includes 15% Cost Increase for Vertical Mounting

GP77-0007-21

FIGURE 39 MECHANICAL POWER TRANSMISSION COMPONENTS AND CHARACTERISTICS

The Giromill rotor blades employ a simple blade design which does not require complexities of twist, camber, and taper associated with most conventional windmill designs. The McDonnell Aircraft Company Producibility department was consulted to obtain raw material and labor costs for rotor blade fabrication. Rotor blades for the 120 kW system identified as configurations 1, 2, and 6, were considered because they offered a wide range of blade span, chord, and weight per unit length. Results from these analyses indicated that total blade cost per unit weight varied only slightly with design. Assuming a manufacturing cost of \$12 per hour, the blade cost of approximately \$4.00/lb was determined.

Blade Control System - The conceptual blade control system utilizes individually modulated blades driven by a control servo motor. The McDonnell Douglas Electronics Company of Grand Rapids, Michigan, was consulted to prepare cost estimates for a rock angle actuator to direct the rotor blades to follow a prescribed rock angle history and provide torque to flip the blades where necessary. Cost estimates for actuators and associated electronics are summarized in Figure 40 for the 120 kW, 500 kW and 1500 kW systems based on recurring cost for the 300th unit, i.e., assuming 3 actuators for each of the 100 Giromills.

Giromill Size (kW)	Estimated Cost per Actuator
120	\$2400
500	\$3400
1500	\$4600

GP77-0007-31

FIGURE 40
ESTIMATED COSTS FOR ROTOR BLADE ACTUATORS

Actuators have been sized with adequate torque for turning the total blade span at each blade station. For the 120 kW system all the blades are in two sections having a support at the one-half span location, and use one control actuator. The 500 and 1500 kW systems, in general, require three or four blade sections separated by supports. In determining these control system costs, two blade control actuators are assumed for Giromill configurations having three or more blade sections, even though only one actuator may be adequate.

Other components of the blade control system include the following sensors and devices:

- ° Control processor
- ° Giromill rpm sensor
- ° Blade angle position sensors
- ° Rotor angle position sensor
- ° Wind velocity sensor and direction sensor
- ° Vibration sensors
- ° Emergency pyrotechnic devices

These components are not affected by Giromill power output, and only slightly affected by the number of blades. A cost of \$10,000 for all three bladed system sizes has been calculated for these components; \$11,000 for four bladed, and \$12,000 for five bladed systems.

8.3 Total Giromill System Cost

The major cost elements for the 120, 500, and 1500 kW systems are summarized in Figure 41. The cost of electrical system components other than generator are assumed to be the same as the generator for the 120 kW system, i.e., \$4025. The cost of the site, site development and security is assumed to be \$15,000 for the 120 kW system and \$30,000 for the 500 and 1500 kW system. In addition, final system installation cost is assumed to be 10% of the total

Element	Material or Description	Cost Factors		
		120 kW	500 kW	1500 kW
Tower Lower and Upper	Carbon Steel Welded or Bolted	\$1.00/lb		
Foundation	Concrete	25% of Tower Cost		15% of Total System Weight
Rotor Blade System Blade Supports Rotor Blades Main Bearings	Tubular Carbon Steel Welded or Bolted Aluminum Diameter of Upper Tower	\$1.00/lb \$4.00/lb \$9 to \$10/lb		
Drive System Couplings Bearings Speed Increaser*	Speed Increaser to Gen., to Drive Shaft Thrust/Radial Bearing on Drive Shaft Price Increases with Gear Ratio	\$4 to \$5/lb \$9 to \$10/lb \$15,000 to \$22,000	\$4 to \$5/lb \$9 to \$10/lb \$26,500 to \$33,000	\$48,300
Electrical Generator*	120 kW (1200 rpm), 500 kW (rpm Optimized for Minimum Generator Plus Speed Incr Cost), 1500 kW (450 rpm)	\$4,025	\$23,000 to \$27,000	\$58,075
Other Components	Control Panel, Gauges	\$4,025	\$4,025	\$4,025
Controls Servo Actuators Other Components	MDEC Grand Rapids Estimate Processor, Sensors, etc.	\$7,200 ⁽¹⁾ \$10,000	\$20,400 ⁽²⁾ \$10,000	\$27,600 to \$46,000 ⁽³⁾ \$10,000 to \$12,000 ⁽⁴⁾
Additional Capital	Installation, Etc. Land Purchase, Site Development, Security	10% of Capital \$15,000	10% of Capital \$30,000	10% of Capital \$30,000
Annual Charges Cost of Capital Operating and Support	Loan Repayment, Depreciation, Bond Interest Stock Dividend, Insurance, Taxes	15% of Total Capital 4% of Total Capital		
Total		19% of Total Capital		

Notes:

* 15% increase in vendor prices for vertical mounting

(1) 3 Actuator at \$2,400 Each

(3) 6 to 10 Actuators at \$4,600 Each

(2) 6 Actuators at \$3,400 Each

(4) Cost of control processor sensors, etc. is \$10,000

for 3 Bladed Configuration, \$11,000 for 4 and \$12,000 for 5

GP77-0007-22

FIGURE 41
COST ESTIMATING RELATIONSHIPS SUMMARY
1975 Dollars

of the subsystem costs. The cost of capital, as shown, is 15% of the total Giromill installed cost, and O&S costs are assumed to be 4% of the total.

Figure 42 presents a summary of the 120 and 500 kW system costs that were reported in our mid-term report using the ground rules and CER's defined in the previous sections.

When the mid-term report was published, the 1500 kW system costs were not yet available. Figures 43 and 44 present the production costs and cost of energy for the 1500 kW systems analyzed. These costs are based on the same ground rules and CER's defined previously with the exception of the main bearing costs. Previously we assumed that the upper and lower main bearings would have the same diameter. Cost analyses showed that the main bearing cost was the single most expensive component for the high power systems. Subsequent structural analyses indicated that the lower main bearing could be substantially reduced in size to about a 1.5 meter diameter. The 1500 kW system costs shown in Figures 43 and 44 are based on having an upper main bearing the size of the tower diameter, and a lower main bearing 1.5 meters in diameter.

8.4 Optimized System Cost

The optimized 500 kW system was costed using the same ground rules and CER's as previously discussed with the exception of:

- (a) The lower main bearing is 1.5 meters in diameter.
- (b) At the suggestion of the Falk Corp., the speed increaser cost increase for a vertical mounting was reduced from 15% to 10%.
- (c) We had previously assumed that the structural steel installed costs were \$1.00 per pound. Consultation with Union Electric utility tower design personnel indicated that they used a value of \$0.50 per pound. Also, a review of the Kaman data presented at their July 1975 Design Review shows that they used \$0.695 per pound. On the basis of this our structural steel cost was reduced from \$1.00 per pound to \$0.75 per pound.

The cost elements for this system were determined and are presented along with the computations in Figure 45. The computations for the cost of energy produced are shown in Figure 46. The results from this single system optimization are quite significant, reducing the cost from 5.62 ¢/kW hr. in our mid-term report down to 4.05 ¢/kW hr. now.

- Mid Term Results Summary
- Configurations 1 Through 7-120 kW
- Configurations 8 Through 15-500 kW

Config No.	Upper and Lower Tower (\$)	Foundation (\$)	Electrical		Power Transmission		Controls (\$)	Main Bearings (\$)	Blade Support (\$)	Rotor Blades (\$)	Total Giromill Cost (\$)	Site Develop and Install (\$)	Total Installed Cost (\$)	Installed Cost (\$/kW)	Power Output			Annual Charges			Energy Cost $\frac{d}{kW\ hr}$
			Gener (\$)	Other (\$)	Speed Increaser (\$)	Other (\$)									Cost of Capital (\$)	O&S (\$)	Total (\$)				
1	37,330	9,332	4,025	4,025	17,500	4,443	17,200	11,400	8,220	21,720	135,195	28,520	163,715	1,364	2,980	357,600	24,551	6,549	31,106	8.70	
2	37,330	9,332	4,025	4,025	19,000	4,443	17,200	11,400	8,330	16,920	12,005	28,201	160,206	1,335	2,980	357,600	24,031	6,408	30,439	8.51	
3	37,330	9,332	4,025	4,025	20,000	4,443	17,200	11,400	8,390	19,000	35,145	28,515	163,660	1,364	2,980	357,600	24,549	6,546	31,095	8.70	
4	31,020	7,755	4,025	4,025	20,300	4,443	17,200	8,200	12,430	15,800	125,198	27,520	152,718	1,273	2,980	357,600	22,908	6,109	29,016	8.11	
5	27,280	6,820	4,025	4,025	22,200	4,443	17,200	5,400	21,050	15,800	128,243	27,824	156,067	1,301	2,980	357,600	23,410	6,243	29,653	8.29	
6	50,350	12,588	4,025	4,025	21,000	4,443	17,200	16,600	13,190	23,320	166,841	31,684	198,525	1,654	3,750	450,000	29,779	7,941	37,720	8.38	
7	29,340	7,335	4,025	4,025	15,000	4,443	17,200	8,800	5,500	12,800	108,468	25,847	134,375	1,119	2,320	278,400	20,156	5,375	25,531	9.17	
8	127,490	31,873	25,000	4,025	26,500	13,865	30,400	162,637	38,780	55,840	516,410	81,641	598,051	1,196	2,980	1,490,000	89,708	23,922	113,630	7.63	
9	134,800	33,700	25,000	4,025	28,500	13,865	30,400	162,637	37,060	67,840	537,827	83,783	621,610	1,243	2,980	1,490,000	93,242	24,864	118,106	7.93	
10	134,800	33,700	25,000	4,025	30,800	13,865	30,400	162,637	36,970	59,200	531,397	83,140	614,537	1,229	2,980	1,490,000	92,181	24,581	116,762	7.84	
11	69,930	17,483	27,000	4,025	30,200	13,865	30,400	72,000	79,100	29,400	373,403	67,340	440,743	881	2,980	1,490,000	66,111	17,630	83,741	5.62	
12	83,550	20,888	27,000	4,025	30,600	13,865	30,400	93,000	60,760	43,720	407,808	70,781	478,589	955	2,980	1,490,000	71,788	19,144	90,932	6.10	
13	200,680	50,170	27,000	4,025	30,800	13,865	30,400	229,997	58,750	77,320	723,007	102,301	825,308	1,651	3,750	1,875,000	123,796	33,012	156,809	8.36	
14	95,840	23,960	23,300	4,025	27,000	13,865	30,400	118,629	24,060	62,920	423,999	72,400	496,399	993	2,320	1,160,000	74,460	19,856	94,316	8.13	
15	155,320	38,830	27,000	4,025	32,700	13,865	20,200	162,637	45,260	85,120	584,959	88,496	673,455	1,347	2,980	1,490,000	101,018	26,938	127,956	8.59	

GP76-0207-1

FIGURE 42
120 kW AND 500 kW GIROMILL SYSTEM COSTS

Config	Upper and Lower Tower \$	Blade Support \$	Rotor ³ Blades (Wt) \$	Total (Wt) \$	Foundation (\$ - 0.15 Wt)	Electrical		Power Transmission		Main Bearings \$	Controls ¹ \$	Total \$
						Generator (450 rpm) \$	Other \$	Speed ² Increaser \$	Other \$			
17	128,690	46,210	(15,460)	(190,360)	28,554	58,075	4,025	48,300	35,000	87,319	37,600	535,613
18	136,590	60,350	(24,300)	(221,240)	33,186						37,600	597,645
19	137,770	65,600	(32,330)	(235,700)	35,355						37,600	638,364
20	139,040	78,400	(23,830)	(241,270)	36,190						46,800	629,469
21	138,040	95,930	(28,190)	(262,160)	39,324						+1,000	676,773
			112,760	346,730							56,000	676,773
											+2,000	

1. Cost of Controller, sensors, etc. \$10,000 for 3 blade configuration, \$11,000 for 4 blade and \$12,000 for 5 blade. Actuator cost at \$4,600 each.

2. Speed increaser cost at \$42,000 x 1.15 - \$48,300 for vertical mounting.

3. Based on using separate work center for high volume, very simple technology.

FIGURE 43
PRODUCTION COST ELEMENTS FOR 1500 kW CONFIGURATIONS

Config	Giromill Cost	Site Develop and Install	Total Installed Cost	Installed Cost (\$/kW)	Specific (hr)	Total kW hr yr	Cost of Capital 15%	O&S 4%	Total 19%	Energy Cost ¢ kW hr
17	535,613	83,561	619,174	412.8	3,100	4,650,000	92,876	24,767	117,643	2.53
18	597,645	89,764	687,409	458.3			103,111	27,496	130,607	2.81
19	638,364	93,836	732,200	488.1			109,830	29,288	139,118	2.99
20	629,469	92,947	722,416	481.6			108,362	28,897	137,259	2.95
21	676,733	97,677	774,450	516.3			116,167	30,978	147,145	3.16

GP77-0007-29

FIGURE 44
COST OF ENERGY PRODUCED FOR 1500 kW CONFIGURATIONS

- (a) Upper and Lower Tower
Total Weight = 60,000 lb
Cost = $0.75 \times 60,000 = \underline{\$45,000}$
 - (b) Foundation
Foundation Cost = $0.25 \times \text{Tower Cost}$
Cost = $0.25 \times \$45,000 = \underline{\$11,250}$
 - (c) Generator and Other Electrical
500 kW Output at 450 rpm
Generator Cost = \$27,000
Other Elect Cost = \$4,025
 - (d) Speed Increaser
Basic Ratio Required = $450/9.6 = 46.9$
Basic Cost = \$29,550
Cost for Vertical Mounting + 10%
Speed Increaser Cost = \$32,505
 - (e) Other Power Transmission Components
Cost = \$13,865
 - (f) Controls
3 Actuators at \$3400 Each + \$10,000 for Control System
Cost = \$20,200
 - (g) Main Bearings
Upper Bearing Diameter = 2.62 m (8.61 ft)
Cost = \$17,500
Lower Bearing Diameter = 1.5 m (5 ft)
Cost = \$5,700
Total Bearing Cost = \$23,200
 - (h) Blade Support
Weight = 57,100 lb
Cost = $0.75 \times 57,100 = \underline{\$42,800}$
 - (i) Blades
Weight = 14,500 lb
Cost = $4 \times 14,500 = \underline{\$58,000}$
- Total Cost (Addition of Underlined Cost Values) = \$277,840

GP77-0007-23

FIGURE 45
500 kW CONFIGURATION 11-1 COST ANALYSIS

- (a) System Cost (from Figure 36) = \$277,840
- (b) Site Development and Installation Cost
 Cost = 10% of System Cost + \$30,000
 Cost = \$57,784
- (c) Total Giromill Installed Cost
 Cost = (a) + (b) = \$335,624
- (d) Installed Cost per kW
 Cost per kW = $335,624/500 = 671$ \$/kW
- (e) Total Power Output
 Power = 1,574,300 kW hr/yr
 Specific Power = $1,574,300/500 = 3149$ hr
- (f) Annual Charges
 Cost of Capital = 15% Installed Cost (c)
 Cost = \$50,343
 Operations and Support = 4% Installed Cost
 Cost = \$13,425
 Total = \$63,768
- (g) Energy Cost (£/kW hr) are Annual Charges (f)
 Divided by Total Power (e) = 4.05 £/kW hr

GP77-0007-28

FIGURE 46
COST OF ENERGY PRODUCED - 500 kW CONFIGURATION 11-1

8.5 Cost Comparison with Conventional Windmills

A cost comparison was made between the Giromill costs and those for a conventional horizontal axis windmill. The cost data for conventional windmills used in this comparison was excerpted from the General Electric and Kaman final presentation charts of their Wind Generator System studies conducted for NASA. The GE charts are dated 17 July 1975, and the Kaman charts are dated 18 July 1975. The comparison is for a 500 kW system. The Giromill system used is configuration 11-1. Figure 47 presents this comparison and shows the Giromill has a lower cost in all categories of installed cost, system cost, and energy cost.

	Conventional Windmill		Giromill
	GE	Kaman	MCAIR
Size	55.8 m (183 ft) dia	45.7 m (150 ft) dia	62.3 m (204 ft) dia by 29.7 m (97 ft) Span
Site Mean Wind, $\bar{V} \sim$ mps (mph)	5.4 (12)	5.4 (12)	5.4 (12)
Rated Wind, $V_R \sim$ mps (mph)	7.27 (16.3)	9.16 (20.5)	8.7 (19.5) (V_{RN})
Annual Energy \sim kW hr	1.88×10^6	1.2×10^6	1.57×10^6
Specific Power \sim hr	3760	2400	3149
Installed Cost \sim \$	486,800	420,500	335,624
System Cost \sim \$/kW	974	841	671
Energy Cost \sim ¢/kW hr	4.18	7.0	4.05

GP77-0007-27

FIGURE 47
GIROMILL AND CONVENTIONAL WINDMILL COST COMPARISON

The energy costs (¢/kW Hr.) depend on the annual charges assumed. The Giromill cost relationship assumed that 19% of the system installed cost was the annual charge. GE and Kaman (from their figures) assumed 16% and 20% respectively. To make the energy costs comparable, the annual charges of the GE and Kaman windmills were related to the annual charge assumed for the Giromill (19%). The results of this are presented in Figure 48. These results show that the energy cost of a conventional windmill is from 21% to 64% more than a Giromill or in terms of a windmill base, the Giromill energy cost is 18% to 39% less than a conventional windmill.

	Conventional Windmill		Giromill
	GE	Kaman	MCAIR
Installed Costs ~ \$	486,800	420,500	335,624
Annual Charge Assumed ~ % of Installed Cost	16	20	19
Resulting Energy Cost ~ ¢/kW hr	4.18	7.0	4.05
Consistent Annual Charge Assumed ~ % of Installed Cost	19	19	19
Comparable Energy Cost ~ ¢/kW hr	4.92	6.66	4.05
Energy Cost in Terms of Giromill Energy Cost	1.21	1.64	1.0

GP77-0007-26

FIGURE 48
ENERGY COSTS COMPARISON FOR A CONSISTANT
ANNUAL CHARGE

9. CONCLUSIONS

A parametric design and cost effectiveness analysis of the 120 kW, 500 kW and 1500 kW Giromill systems has been completed. Cost effectiveness trends with system size and rated wind speed exhibit similar trends observed with conventional windmills.

The design groundrules used in the Giromill study were similar to those used in the conventional windmill studies so that direct comparisons between systems is valid.

The design criteria, construction techniques, materials and hardware components used for the Giromill design are all state-of-art or can be procured off the shelf at this time. No new or innovative techniques need be developed.

A 500 kW Giromill system has been optimized to provide for the lowest energy cost. This system has an energy cost of 4.05 ¢/kW hr. which is 18% to 39% less than the comparable conventional windmill costs estimated by GE and Kaman.

The Giromill system rotor performance was based on the analytical results obtained using the cyclogiro vortex theory computer program. Since the cost of power produced by the Giromill is based on rotor performance, a test to verify the performance predictions should be undertaken.

APPENDIX A

HIGH WIND GROUNDRULE ANALYSIS

The initial study results were analyzed to determine if any of the ground rules had a strong influence on the Giromill design. The one having the greatest affect was the high wind condition. The ground rule assumes that a 54 mps (120 mph) wind exists at a height of 9 meters (30 ft.). Up rating this wind to a height of 30 meters (100 ft.) using the 1/7 power law results in a wind of 64 mps (142.5 mph) which was used for design purposes. The high wind condition designed the blade support arms and the upper and lower tower. The upper tower had the greatest impact on cost because the tower diameter establishes the diameter of the upper main bearing, and this bearing is one of the major cost items.

An investigation was conducted to determine the cost impact of reducing the high wind to 54 mps (120 mph), acting at 30 meters, instead of 64 mps. The method employed was based on the technique outlined in Reference 3, "Handbook of Geophysics and Space Environments," Section 4.5.2, Extreme Surface Wind Speeds. The method was applied to the wind data from Abilene, Texas, which has one of the highest mean wind and standard deviation in the U.S. The values for a height of 50 ft. are:

Extreme annual mean wind - 28 mps (63 mph)

Standard deviation - 6.1 mps (13.6 mph)

Average greatest wind speed to be expected in 30 years - 45 mps (100 mph).

Applying these data resulted in the statistics shown in Figure A1 for the Giromill design high wind at a height of 30 meters.

Abilene, Texas Winds Assumed		
<u>Design Wind at 30 meters</u>	<u>30 Years Risk¹</u>	<u>Return Period²</u>
64 mps	3.2%	900 Years
54 mps	20%	120 Years
¹ Probability of being exceeded in 30 years time. ² Period in which design wind is expected to be exceeded one or more times.		

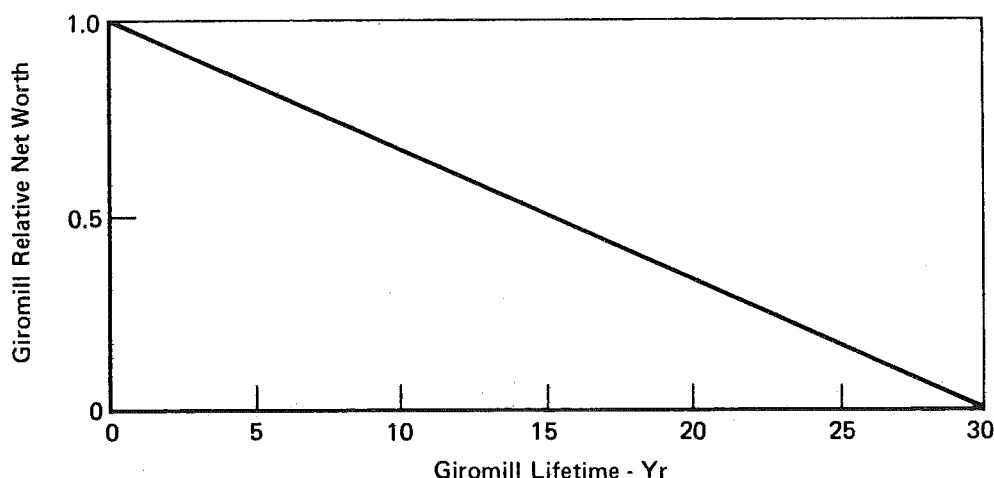
GP77-0007-24

FIGURE A1
GIROMILL DESIGN WIND STATISTICS

Assuming that the risk probability is due to a tornadic type wind, so that any high wind that can destroy a Giromill occurs in an isolated (independent) area, the risk value can be equated to the number of Giromills destroyed. Over 30 years, 32 Giromills out of every thousand designed for a 142.5 mph wind would be destroyed and 200 of those designed for 120 mph winds.

Giromills destroyed late in their life (after 20 to 25 years of service) would not be worth very much. To account for this in the cost trade off analysis, it was assumed that Giromill worth is linear with time, decreasing from 1.0 at time zero, to zero at time 30 years as shown in Figure A2. The total cost in terms of equivalent new Giromills to keep 1000 of them operating for a minimum of 30 years is therefore:

$$\text{Equivalent Number of New Giromills} = (\text{Original number initially bought}) + (\text{Number lost}) \times (\text{Average relative net worth of Giromills lost})$$



Equivalent Number of New Giromills

$$54 \text{ mps Design Wind} = 1000 + 200 \times 0.5 = 1100$$

$$64 \text{ mps Design Wind} = 1000 + 32 \times 0.5 = 1016$$

GP77-0007-25

FIGURE A2
GIROMILL WORTH OVER 30 YEARS

The calculations are detailed in Figure A2 and show that one must buy 1100 equivalent new Giromills designed for 54 mps winds, and 1016 equivalent new Giromills designed for 64 mps winds. This means that if the cost of the 54 mps design wind Giromill is less than 92% (1016/1100) the cost of a 64 mps Giromill, it is more cost effective to obtain the lower design wind units.

The validity of this method of taking into account the design high wind in the cost effective analyses is not known, but this example problem does point out that all ground rules should be carefully defined and supported by sufficient trade off studies to assure the most cost effective design is selected.

REFERENCES

1. Brulle, R. V., et.al., "Feasibility Investigation of the Giromill for Generation of Electrical Power, Mid-Term Report," ERDA Report COO-2617-75/1, dated 1 November 1975.
2. Summary of Airfoil Data, NACA TR 824, 1945.
3. Handbook of Geophysics and Space Environments, Published by Cambridge Research Lab, 1965.